Behavior and Design of Concrete Filled Tubular Columns Exposed to Fire

Taddhanpally Shashank

A Dissertation Submitted to
Indian Institute of Technology Hyderabad
In Partial Fulfillment of the Requirements for
The Degree of Master of Technology/ Doctor of Philosophy

भारतीय प्रौद्योगिकी संस्थान हैदराबाद
Indian Institute of Technology Hyderabad

Department of Civil Engineering

July, 2016

Declaration

I declare that this written submission represents my ideas in my own words, and where others' ideas or words have been included, I have adequately cited and referenced the original sources. I also declare that I have adhered to all principles of academic honesty and integrity and have not misrepresented or fabricated or falsified any idea/data/fact/source in my submission. I understand that any violation of the above will be a cause for disciplinary action by the Institute and can also evoke penal action from the sources that have thus not been properly cited, or from whom proper permission has not been taken when needed.
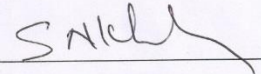
_____

(Signature)

_____

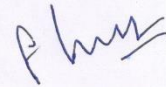Taddhanpally Shashank

_____

CE14MTECH11009

Approval Sheet

This thesis entitled "**Behavior and Design of Concrete Filled Tubular Columns Exposed to Fire**" by T. Shashank (CE14MTECH11009) is approved for the degree of Master of Technology from IIT Hyderabad.
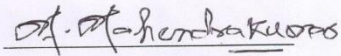
Dr. Anil Agarwal
Adviser

Dr. Syed Nizamuddin Khaderi
External Examiner

Dr. S. Suriya Prakash
Internal Examiner

Dr. Mahendrakumar Madhavan
Internal Examiner

Acknowledgements

Abstract

Concrete filled tubular (CFT) columns have become increasingly used in recent decades, due to their excellent structural performance, which takes advantage of combined steel and concrete working together. Using the steel and concrete together provides a series of advantages: high load carrying capacity, aesthetic appearance, increases the floor area and efficient construction technology are widely known benefits.

Circular, Square, and rectangular hollow sections are mostly used to form these composite columns. Now-a-days elliptical sections are also introduced into the composite sections. Researchers are also focusing on the double-skin CFT columns to increase fire resistance capacities. In this thesis Square, rectangular and the circular sections are studied.

The behavior of the CFT columns at room temperature are well established in the last years. But in case of fire situation the degradation of material properties gives rise to an extremely non-linear behavior of these CFT columns, which makes difficult to predict their failure. In this thesis fire behavior of the CFT columns is reviewed and the design equations proposed by the researchers is studied against their accuracy. It is stated that further investigation is needed for a complete understanding of performance of CFT columns in the fire situation.

In this thesis fire behavior of CFT columns is studied by means of realistic three dimensional finite element model. Accuracy of Numerical models is verified against the experimental results. Material properties for both the steel and concrete at the elevated temperatures are taken from Eurocode 1994 and Lie (1996). Parametric studies were carried out to determine factors which influence the behavior of the CFT columns exposed to fire. The Scope of this thesis is restricted to CFT columns subjected to concentric axial loads.

Nomenclature

f_{cu} Concrete cubic strength

fy   Yield strength of steel tube

B   Width of rectangular section

D   Depth of rectangular tube

A_s Steel cross sectional area

A_c Concrete cross sectional area

e   Eccentricity of load

a   Fire protection thickness

E_c Concrete modulus of elasticity

E_S Steel modulus of elasticity

L   Length of column

N_u Ultimate strength of composite columns at ambient temperature

$N_u(t)$ Strength of the composite columns corresponding to the fie duration

               time(t)

β   Depth to width ratio of rectangular steel tube (D/B)

R   Fire resistance period in minute

T   Temperature in ^oC

t	Thickness of steel tube
$(\Delta l/l)$	Thermal elongation
N	Applied load
θc	Temperature of concrete in $^{\circ}$C
λ_a	Thermal conductivity of steel
λ_c	Thermal conductivity of concrete
c_a	Specific heat of steel
c_c	Specific heat of concrete
α_a	Thermal expansion coefficient of steel
α_c	Thermal expansion coefficient of concrete

Abbreviations

CFT	Concrete filled tube
CHS	Circular hollow section
EC1	Eurocode 1 Part 1-2 (EN 1991-1-2)
EC2	Eurocode 2 Part 1-2 (EN 1992-1-2)
EC3	Eurocode 3 Part 1-2 (EN 1993-1-2)
EC4	Eurocode 4 Part 1-2 (EN 1994-1-2)
HSC	High strength concrete

P-P   Pinned-pinned supporting conditions

F-F   Fix-Fix supporting conditions

RSI   Residual strength index

FEM   Finite element modelling

FEA   Finite element analysis

Contents

List of Figures

List of tables

Chapter 1

Introduction

1.1. Background

Concrete-Steel composite sections are widely used in the U.S, China, Japan and many foreign countries because of they combine the advantages of both the steel and concrete properties. Generally composite sections offer a greater resistance to the deformations against the applied loads and they tend to improve the load carrying capacity. Composite sections that are used in the constructions include composite slabs, composite beams, composite columns.

1.2. Types of Composite Columns

Composite columns are available in many different types of cross-section. Some of them are shown in the below figure. Steel encased in concrete is one of the oldest type of the composite column. Due to the low grade of concrete in the past they used steel encased concrete column to provide insulation to the steel section during fire. But later on these sections were replaced by the concrete filled tubular columns which eliminates the requirement of form work and there is no need of separate reinforcement. The construction speed increases using the CFT columns.
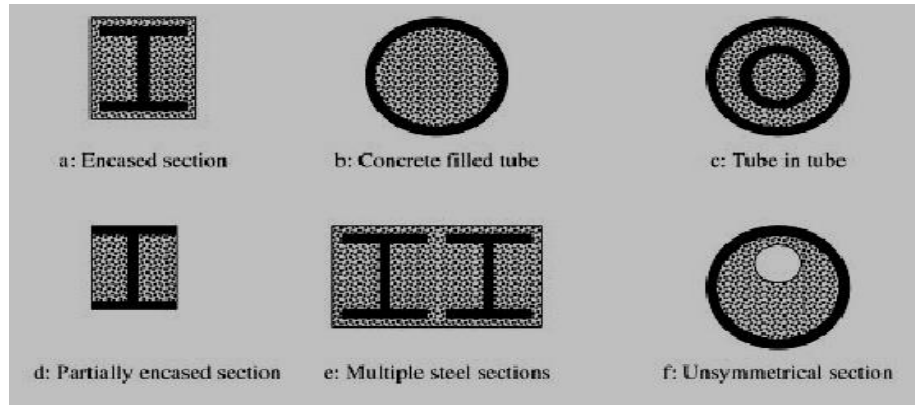
Figure 1.1. Types of composite columns

Ref: Textbook on Composite columns by David Nethercot

1.3. Concrete filled Tubular columns

Concrete filled tubular (CFT) column consist of a steel encased reinforced column which may be of square, rectangular or circular shape. The presence of the steel on the concrete boundary increases the load carrying capacity of the column. Also the steel framework acts as a formwork for placing the concrete. CFT columns are more efficient because the steel tube confines the concrete infill and the concrete infill prevents the local inward buckling of the steel tube. The presence of the fire on the CFT columns is discussed in this research. CFT columns provide better fire resistance properties than the normal reinforced columns. By providing the additional fire protection thickness on the steel surface increases the fire resistance of the column. But the cost of the column may be increased substantially if we provide the fire protection on the steel surface.

CFT structural member has distinct advantages over an equivalent steel, reinforced concrete, steel reinforced concrete member. The orientation of steel and concrete in the cross section optimizes the strength and stiffness of the section. The steel lies at the outer perimeter where it effectively resists the tension and the bending moment. The stiffness of the CFT is greatly

enhanced because of steel which has greater modulus of elasticity than the concrete. The location

of steel is farthest from the centroid in the CFT, where it makes greatest contribution to the moment

of inertia. The concrete forms an ideal core which increases the compressive strength and prevents

the local buckling of the steel. In contrast to reinforced columns with transverse reinforcement the

steel tube in the CFT prevents the spalling of the concrete. Depending on cross-sectional shape

CFT columns are classified into square, circular and polygonal CFT columns.
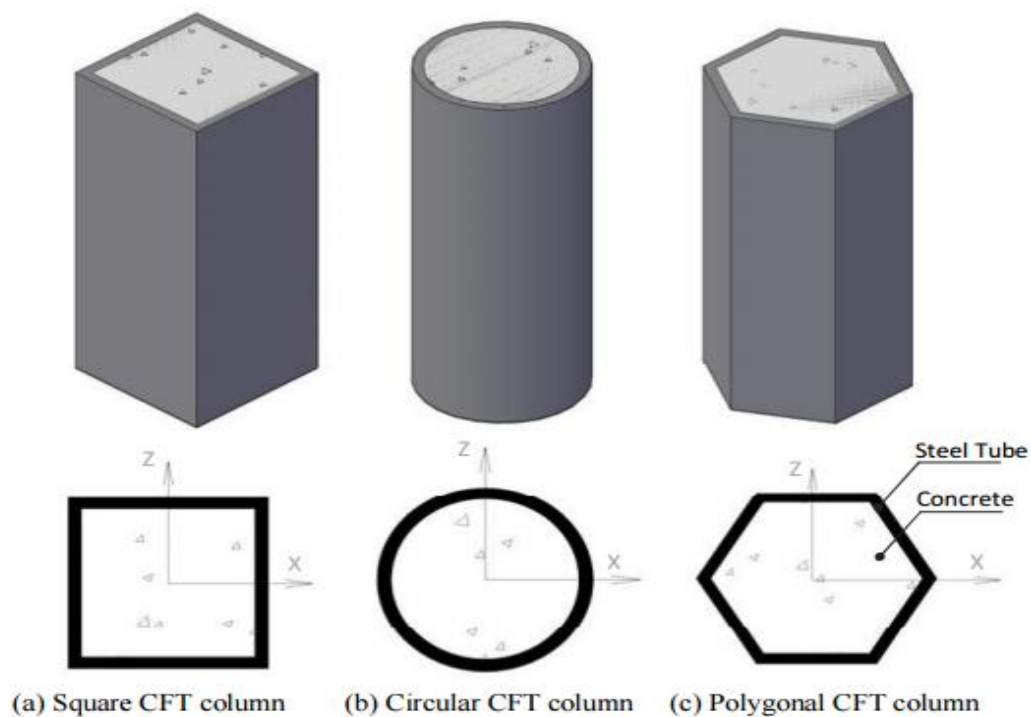
Figure 1.2. Types of CFT columns

1.4. Practical applications of CFT Columns

The use of concrete filled steel tubes has increased in recent decades, finding an important demand in the construction of high rise buildings and bridges. Other applications include electricity transmitting poles, subways or office blocks etc.

An example of high-rise buildings using CFT column can be found in China (Zhao et al. 2010). The SEZ plaza in Shenzhen, which is the tallest building in china using composite columns, is a 76-storey office block with a four level basement and a total height of 361m. It employs CFT columns of circular shape with diameters ranging from 9000 to 1600 mm. In the construction of building, up to two-and-a-half storeys were erected per week, which clearly demonstrates the efficiency of this technology. Another example is Wuhan International security building (WISB), which uses CFT columns of square and rectangular sections, reaching a height of 249.2 m. More than 100 bridges using this type of composite section s have been constructed in china. Similarly there are many constructions in Japan which used CFT columns. An example is the Nakanoshima Intes building (Osaka), which is an office building of 22 storeys height built using the circular and square CFT columns of width/diameter ranging from 600 to 850mm.

IN U.S CFT columns were used in the Museum of Flight at King Country Airport (Seattle, Washington) which used bar-reinforced concrete filled CFT columns for supporting the roof of exhibit hall, which permitted to achieve required fire protection without the need for external sprayed fire protection. At the same time it provided aesthetic finishing and minimized the use of space and allowing for a clean entrance of natural light.

Figure 1.3. Fleet Place House (London, UK) [Espinos 2011]

Fleet place House is a eight-storey office block using circular CFT columns of 323.9 mm external diameter filled with concrete of grades C40 to C60.

Figure 1.4. Millennium Tower (Wien, Austria) [Espinos 2011]

Millennium Tower in Wein is a high rise building of 55 storey height built using concrete filled tubular columns in combination with other composite elements.

1.5. Fire behavior of typical CFT columns

Filling the steel hollow sections with concrete provides the column a high inherent fire resistance without the need of additional protection. During the initial stages of fire exposure, the steel tube expands faster than the concrete core, in such a way that the steel section carries higher load than the concrete core. The heat gets transferred from the steel to concrete core which has lower thermal conductivity. The temperature rise in concrete is very slow and after a period of around 20-30 minutes the strength of steel starts to decrease due to its elevated temperature (Ana Espinos, 2012). At this stage the load gradually gets transferred to the concrete infill. As the temperature advances through the concrete core its strength decreases until it eventually fails either due to buckling or compression.
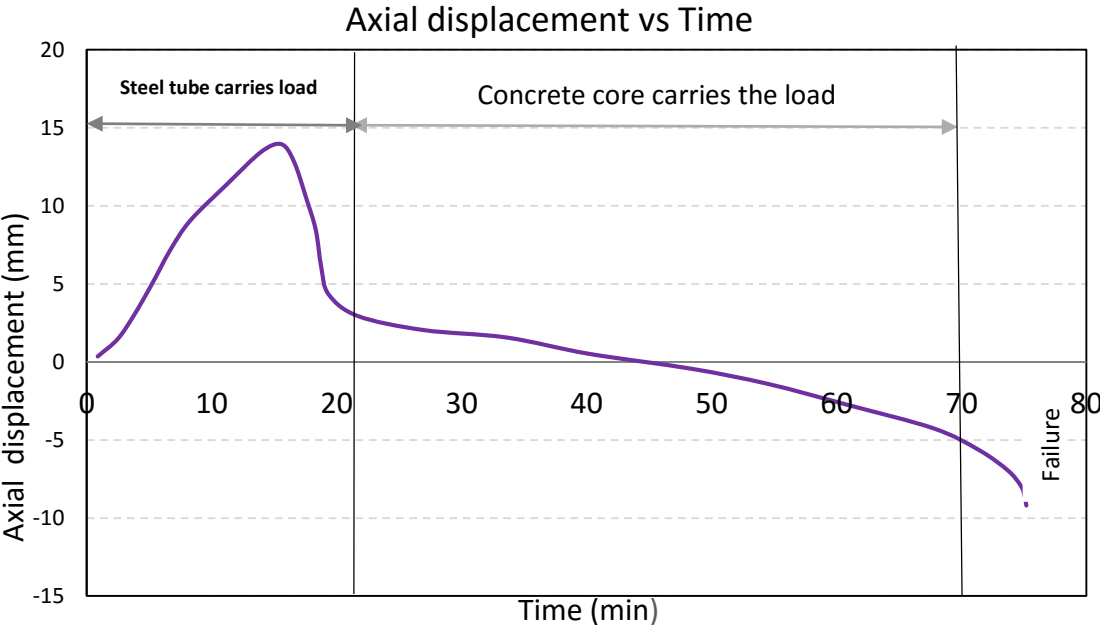
Figure 1.5. Typical behavior of CFT exposed to fire Espinos (2012)

Chapter 2

STATE OF THE ART AND PRIOR

INVESTIGATIONS

The current research in the fire behavior of CFT columns is reviewed covering from the more simpler numerical models to the advanced models which brought the advances in the evaluation of fire resistance of CFT columns, with investigation of the experimental studies helped to promote the use of this technology and finding the recent technology and advances in predicting the fire behavior of CFT columns.

2.1. Experimental Investigations

A large number of fire testing programs have been carried out world-wide on CFT columns since early 80's. Initial researches on the CFT columns mainly focused on the plain or bar reinforces CFT columns subjected to the concentric loads. After some time they focussed on the eccentrically loaded columns, and the other types of infill like fiber reinforced concrete or high strength concrete for increasing the fire resistance of CFT columns. But now-a-days other section shapes are investigated like double skin steel tubular columns and also post-fire behavior of CFT columns is being studied.

The first tests on CFT columns can be found in a publication AFMFIC 1917. But specific fire testing programs never appeared over a very long time. The fire behavior of composite hollow section columns was investigated for the first time in a research work sponsored by CIDECT

(Comite International pour le Development et lEtude de la Construction tubulaire). Between the years 1974 and 1982, several experimental programs were carried out (COMETUBE 1976, Gradjean et al. 1980, Kordina & Klingsch 1983) in the framework of this research.

The CIDECT research project 15A (COMETUBE 1976) consisted of 75 tests on square concrete filled steel tubular columns, with the exception of one test carried on a circular hollow section column. 50 columns were filled with ordinary concrete, 19 with reinforced concrete and 6 columns were tested as empty. The sectional dimensions of the columns varied from 140mm to 225mm and the length of the column was 3600 mm. These tests were carried out at Maizieres-les-Metz and Champs-sur-Marne (France).

Researchers from the Institute for Research in Construction at the National Research Council of Canada (NRCC) carried out several experimental programs between the years 1982 and 1994 (Lie & Chabot 1992, Kodur & Lie 1995), testing CFT columns of circular and square sections filled with bar-reinforced, plain, steel-fiber reinforced concrete. The tested columns had the sectional dimensions ranging from 141.3 to 406.4 mm, steel tube thickness varying from 4.78 to 12.70 mm, and a constant length of 3810 mm. The columns were tested under the fixed end conditions and subjected to concentric axial load, except the two cases were the effect of eccentricity was studied. Concrete mixes with 28-day cylinder strength varied between 23 MPa and 43 MPa. The percentage of reinforcement was 2.3% for bar reinforced and steel-fiber reinforced columns it was around 1.76% by mass.

Some tests on high strength concrete filled tubular columns were carried out after a time in the NRCC facilities (Kodur & Latour 2005). Six circular and two square CFT columns filled with high strength concrete were tested. The diameters of the circular columns varied from 219.1 mm to 406.4 mm, while the width of the square sections was fixed to 203.2 mm. The

concrete strength at 280 days varied from 68.4 to 90 MPa. The length of the columns was 3810 mm.

In the last few years, a great number of fire tests have been carried out in Fuzhou University (China) by the research group headed by professor Han (Han & Huo 2003, Han et al. 2003 a, b, Han & Lin 2004, Han et al. 2005). The research group obtained the results of residual strength of CFT columns after the exposure to the standard fire. Some tests were also carried out by the same research group on slender columns (Han et al .2003 a). In this program, 13 slender CFT columns of circular4 section were tested, 5 of them are externally protected. The columns had a length of 3810 mm. The parameters investigated are cross-section, steel wall thickness, fire protection thickness and load eccentricity.

Romero et al. (2011) presented the results of an experimental program on slender axially loaded CFT columns subjected to fire, carried out in the testing facilities of AIDICO in Valencia (Spain). The aim of the testing program was to investigate the effects of three main parameters of fire behavior of these columns: concrete strength, type of infilling and the axial load level. Normal (NSC) and high strength concrete (HSC) mixtures were employed. Sixteen fire tests were carried on the circular columns which are of length 3810 mm and cross section of 159*6 mm.

Ana Espinos (2012) presented the results of circular CFT columns of length 3810mm conducted by Lie and Chabot (1992). The axial load was applied through the plate attached at the end. Due to this the expansion of steel takes place and during the first 20-30 min the steel alone carries the entire load. The outer dimension of the column was varied from 141.3 mm to 273.1 mm. Further concrete filled elliptical hollow sections are studied and validated with the experimental results.

Chapter 3

Design Equations on CFT columns exposed to fire

Design equations were proposed by the Researchers which predicts the fire resistance of the CFT columns. But there were some restrictions to these equations and can't merely applied to every columns exposed to fire. Some of the design equations which are developed are as given below:

3.1. *Simplified design equation proposed by Kodur*

Kodur (1996) proposed a simplified equation based on the results of parametric studies supported by an experimental program carried out in the institute for research in Construction, NRCC, Canada (Lie and Chabot, 1992, Chabot and Lie, 1992, and Kodur and Lie, 1995) on square and circular CFT columns under fire. This approach is used in the U.S and Canada after incorporating into several building codes (ASCE 1999, NBCC 2005, ACI 2007) and design guides (Ruddy et al. 2003). Kodur's equation directly gives the fire resistance of the CFT column in minutes as a function of different parameters such as column diameter, effective length, type of concrete filling, cross-sectional shape, concrete strength, and percentage of reinforcement.

The fire resistance time of the column can be evaluated by the following equation:

$$R = f\left(\frac{f_c + 20}{KL - 1000}\right) D^2 \sqrt{\frac{D}{N}}$$

Where, R is the Fire resistance in minutes, f_c is the concrete strength at the age of 28 days in MPa, D is the outside diameter/width of the column, N is the applied load in KN, KL is the effective length of the column and *f* is the coefficient which includes the effect of rest of parameters, given in Kodur (1999).

Table 3.1. Values of factors for the corresponding aggregate and cover thickness (Lie 1996)

Aggregate type	Percentage of steel reinforcement	Concrete cover thickness (mm)	Values of f_1 (For circular columns)	Values of f_2 (For square columns)
Siliceous	<3%	<25	0.075	0.065
Siliceous	<3%	≥25	0.08	0.07
Siliceous	≥3%	<25	0.08	0.07
Siliceous	≥3%	≥25	0.085	0.075
Carbonate	<3%	<25	0.085	0.075
Carbonate	<3%	≥25	0.09	0.08
Carbonate	≥3%	<25	0.09	0.08
Carbonate	≥3%	≥25	0.095	0.085

Ref: Lie & Kodur (1996)

Table 3.2. Comparison of fire resistance against the equation

Sectional dimension (mm)	End condition	f_y (MPa)	E_s (*10^5) (MPa)	f_{cu} (MPa)	Test load (kN)	e/r	Exp (min)	Model (min)	Equation (min)
350*350*7.70	Fix-Fix	284	1.83	18.7	2700	0	140 [**504ºC**][#]	109 [**455ºC**][#]	92.5

350*350*7.70	Fix-Fix	284	1.83	18.7	1670	0.3	109 [**586ºC**] [#]	93 [**545ºC**] [#]	-----

[#]Temperature of steel surface at failure

3.1.1. Limitations of this equation:

1) The equation is applicable only to ASTM E119 standard temperature, but it maynot predict the fire resistance incase of real fires and gradual fires.

2) This equation is applicable only to the unprotected CFT column, incase of the protected CFT columns it is not applicable.

3) This equation is applicable to uniform fire (4-sided), but in case of non-uniform fire (3-sided) it is not applicable.

4) For eccentrically applied load this equation can't be used.

3.2 Strength index proposed by Han et al.

Han and co-workers (Han et al. 2003) proposed a formulation to determine the strength index of circular CFT columns filled with plain concrete. Based on the results of parametric studies experimental studies carried out at the Tianjin Fire Research Institute (China). The formulation was obtained by regression analysis, and is valid for circular CFT columns without fire protection and exposed to fire. They also developed design equations for columns with external fire protection and incorporated into the Chinese code DBJ13-51 (DBJ 2003).

The Strength Index is defined as:

$$SI = \frac{N_u(t)}{N_u} = \begin{cases} \dfrac{1}{1+a.to\wedge 2.5}, & t_o \leq t_1 \\[3mm] \dfrac{1}{b.to+c}, & t_1 < t_o \leq t_2 \\[3mm] k.t_o+d, & t_o > t_2 \end{cases}$$

Where, $N_u(t)$ is the ultimate strength of the column corresponding to the fire resistance time (t) and N_u is the ultimate strength of the column at room temperature, $t_o = t/100$, t_1 and t_2 are the transition times depending on the value of $D_o = D/600$ and $\lambda_o = \lambda/40$. *a, b, c, d, k* are the regression coefficients which also depend on D_o, λ_o, and t_1, t_2. For simplicity the definition of different coefficients are not presented here, but it can be found at Han et al. (2003).

The validity of the above equation are $t \leq 180$ min, D=150 - 200 mm, f_y=200-500 MPa, f_c =20 – 60 MPa and λ=15 - 80 (Slenderness ratio). And also this equation is applicable to the standard fires.

3.3 Design equations from Eurocode (1994-1-2)

The Eurocode (1994-1-2) provides two different methods for calculating of compressive load carrying capacity of a CFT column exposed to fire loading. Both these methods require dividing the cross-section into a number of fibers. Similarly, both of these methods assume complete composite cation between the steel and the concrete components. The first (simpler) method uses the column capacity curves available for steel columns, where as the second method (more complex) requires the calculation of the tangential stiffness of the cross- section

Chapter 4

Development of Numerical Model

4.1. Material behavior at elevated temperature

4.1.1 Thermal properties of concrete at elevated temperatures

4.1.1.1 *Formulation from Eurocode 2*

Eurocode 2 part 1.2 (CEN 2004a) describes in its section the thermal properties of concrete at elevated temperatures.

Thermal elongation

The thermal elongation of concrete $(\Delta l/l)_c$ may be determined from the following equations.

Siliceous aggregates:

$$(\Delta l/l)_c = -1.8*10^{-4}+9*10^{-6}*\theta c+2*3*10^{-11} *\theta c^3 \qquad \text{for } 20ºC \leq \theta c \leq 700ºC$$

$$(\Delta l/l)_c = 14*10^{-3} \qquad \text{for } 700ºC \leq \theta c \leq 1200ºC$$

Calcareous aggregates:

$$(\Delta l/l)_c = -1.2*10^{-4}+6*10^{-6}*\theta c+1*4*10^{-11} *\theta c^3 \qquad \text{for } 20ºC \leq \theta c \leq 805ºC$$

$$(\Delta l/l)_c = 12*10^{-3} \qquad \text{for } 805ºC \leq \theta c \leq 1200ºC$$
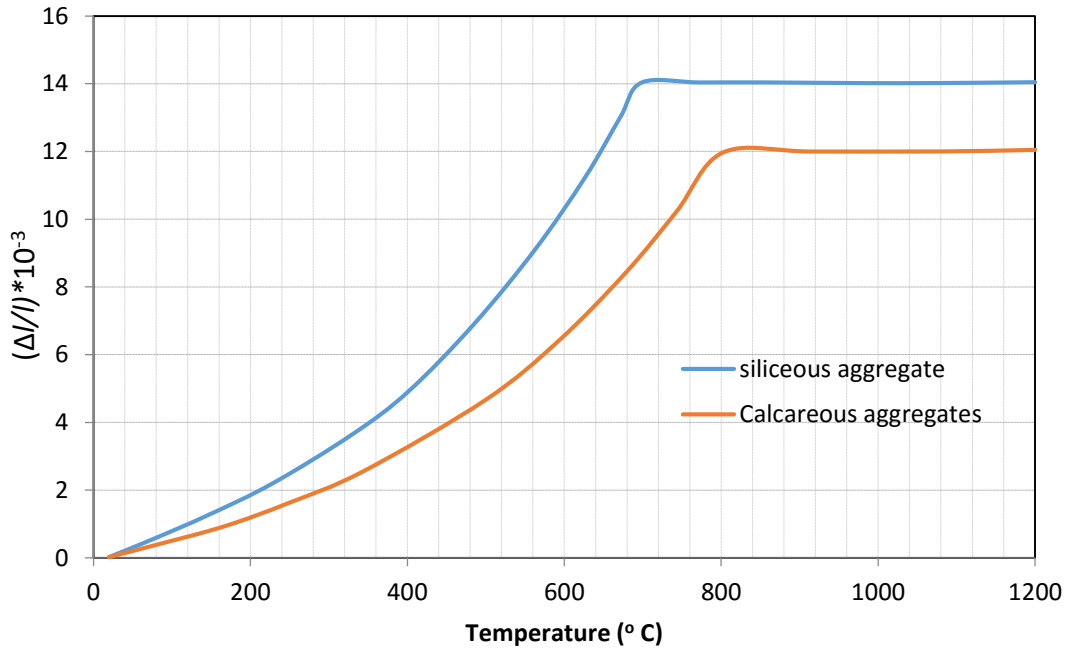
Figure 4.1 Thermal elongation of concrete at elevated temperature (EC3 2005b)

Specific heat

The specific heat is determined from the following equations:

$C_c = 900$ (J/kgK) for $20°C \leq \theta c \leq 100°C$

$C_c = 900 + (\theta c - 100)$ (J/kgK) for $100°C \leq \theta c \leq 200°C$

$C_c = 1000 + (\theta c - 200)$ (J/kgK) for $200°C \leq \theta c \leq 400°C$

$C_c = 1100$ (J/kgK) for $400°C \leq \theta c \leq 1200°C$

Thermal conductivity

Upper limit:

$\lambda_c = 2 - 0.2451 \cdot (\theta c / 100) + 0.0107 \cdot (\theta c / 100)^2$ (W/mK) for $20°C \leq \theta c \leq 1200°C$

Lower limit:

$$\lambda c = 1{,}36 - 0.136 \cdot (\theta c /100) + 0.0057 \cdot (\theta c /100)^2 \ \ (\text{W/mK}) \qquad\qquad \text{for } 20^\circ \text{ C} \le \theta c \le 1200^\circ \text{ C}$$

EC4 Part 1-2 3.3.2(9) recommends the use of the upper limit for steel concrete composite members.
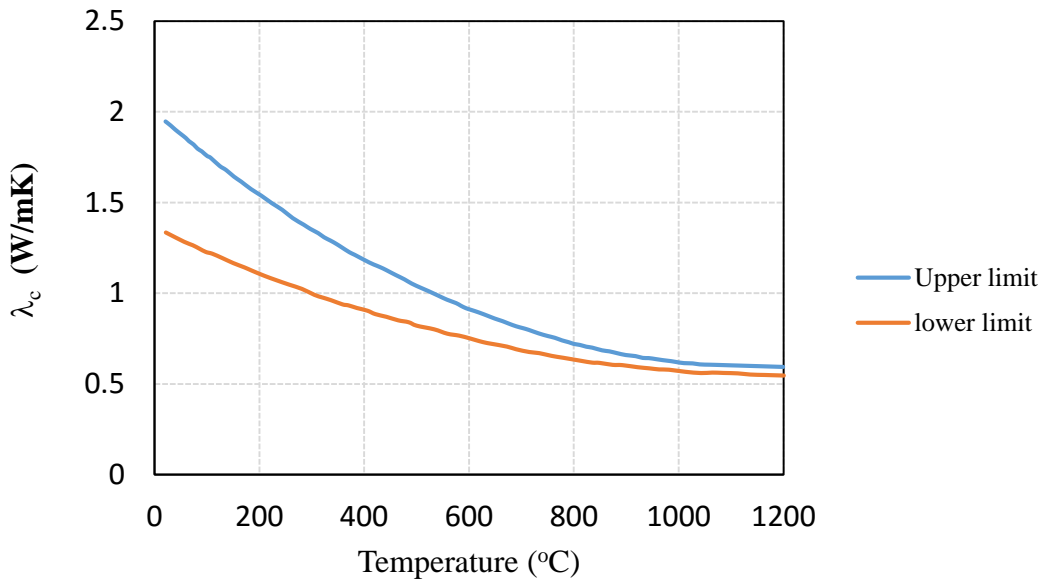
Figure 4.2. Thermal conductivity of concrete at elevated temperature (EC3 2005b)

4.1.1.2 Formulation from lie

Lie (1984) have proposed different formulations for the thermal properties of concrete at elevated temperatures.

Thermal capacity

The thermal capacity of concrete $\rho_c . c_c$, may be determined by means of following expressions:

$\rho_c.c_c = 2.566.10^6$ (J/m^3 °C)   for $0°C \leq \theta_c \leq 400°C$

$\rho_c.c_c = (0.1765.\theta_c - 68.034).10^6$ (J/m^3 °C)   for $400°C < \theta_c \leq 410°C$

$\rho_c.c_c = (-0.05043.\theta_c + 25.00671).10^6$ (J/m^3 °C)   for $410°C < \theta_c \leq 445°C$

$\rho_c.c_c = 2.566.10^6$ (J/m^3 °C)   for $445°C < \theta_c \leq 500°C$

$\rho_c.c_c = (0.01603.\theta_c - 5.44881).10^6$ (J/m^3 °C)   for $500°C < \theta_c \leq 635°C$

$\rho_c.c_c = (0.16635.\theta_c - 100.90225).10^6$ (J/m^3 °C)   for $635°C < \theta_c \leq 715°C$

$\rho_c.c_c = (-0.22103.\theta_c + 176.07343).10^6$ (J/m^3 °C)   for $715°C < \theta_c \leq 785°C$

$\rho_c.c_c = 2.566.10^6$ (J/m^3 °C)   for $\theta_c > 785°C$

Where, for θ_c is the temperature of concrete in °C

Thermal conductivity

The thermal conductivity of concrete λ_c , may be obtained from the following equations:

$\lambda_c = 1.355$ (W/m°C)   for $0° C \leq \theta_C \leq 293° C$

$\lambda_c = -0.001241*\theta_C + 1.7162$ (W/m°C)   for $\theta_C > 293°C$

Where, θ_C is the temperature of concrete in ^{0}C.

Thermal expansion coefficient

The thermal expansion coefficient of concrete α_c is given as,

$\alpha_C = (0.008 \cdot \theta_c + 6)*10^{-6}$ (m/m°C)

Where, θ_C is the temperature of concrete in ^{0}C.

17

4.1.2. Thermal properties of Steel at elevated temperatures

4.1.2.1 Formulation from Eurocode 3

Eurocode 3 part 1.2 (CEN 2005b) describes in its section 3.4 the thermal properties of steel at elevated temperatures. The same definition of properties were included in EC part 1.2 (CEN 2005c) with some minor changes.

Thermal elongation

The thermal elongation of steel $(\Delta l/l)_a$ may be determined from the following equations:

$(\Delta l/l)_a = 1.2.10^{-5}.\theta_a + 0.4.10^{-8} - 2.416.10^{-4}$ for $20^\circ\,C \leq \theta_a \leq 750^\circ\,C$

$(\Delta l/l)_a = 1.110^{-2}$ for $750^\circ\,C \leq \theta_a \leq 860^\circ\,C$

$(\Delta l/l)_a = 2.10^{-5}\theta_a - 6.2.10^{-3}$ for $860^\circ\,C \leq \theta_a \leq 1200^\circ\,C$
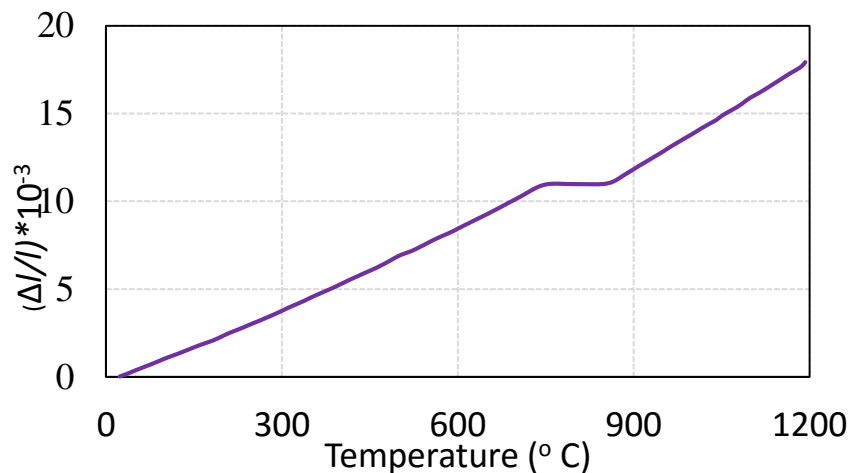
Figure 4.3. Thermal elongation of concrete at elevated temperature (EC3 2005b)

Specific heat

The specific heat of steel, c_a is given by the following equations:

$c_a = 425 + 7.73 \cdot 10^{-1} \cdot \theta_a - 1.69 \cdot 10^{-3} \cdot \theta_a^3 + 2.22 \cdot 10^{-6} \cdot \theta_a^3$ (J/kgK)   for 20° C $\leq \theta_a \leq 600^\circ$ C

$c_a = 666 + \dfrac{13002}{738 - \theta a}$ (J/kgK)   for 600° C $\leq \theta_a \leq 735^\circ$ C

$c_a = 545 + \dfrac{17820}{\theta a - 731}$ (J/kgK)   for 735° C $\leq \theta_a \leq 900^\circ$ C

$c_a = 650$ (J/kgK)   for 900° C $\leq \theta_a \leq 1200^\circ$ C

where, θ_a is the temperature of steel in $^\circ$ C
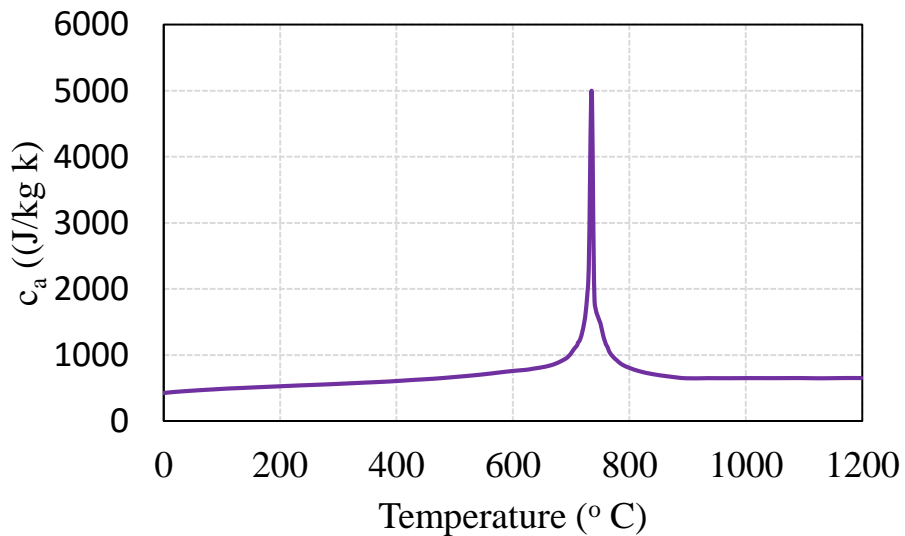
Figure 4.4. Specific heat of steel at elevated temperature (EC3 2005b)

Thermal conductivity

The thermal conductivity of steel, λ_a is determined by the given equations:

$\lambda_a = 54 - 3.33.10^{-2}.\theta_a$ (W/mK)   for $20^\circ\,C \le \theta_a \le 800^\circ\,C$

$\lambda_a = 27.3$ (W/mK)   for $800^\circ\,C \le \theta_a \le 1200^\circ\,C$

Where, for θ_a is the temperature of steel in $^\circ$C.
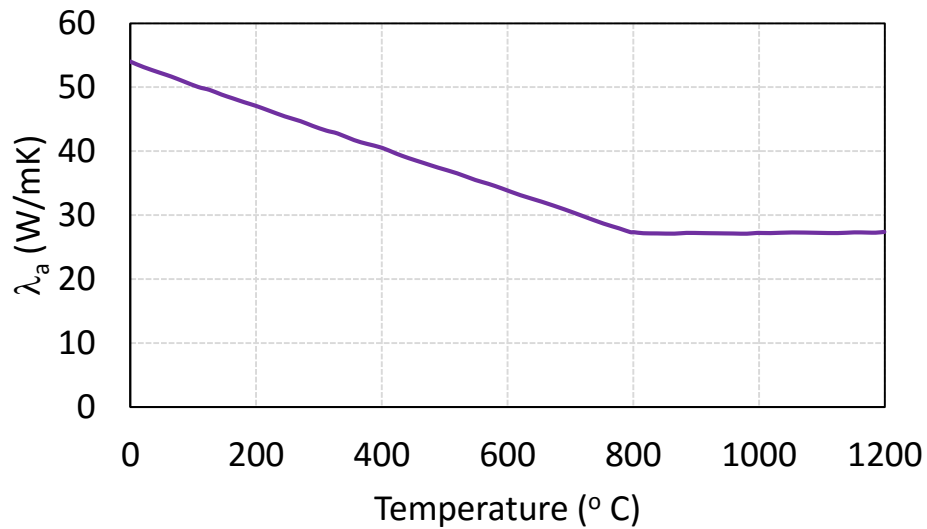
Figure 4.5. Thermal conductivity of steel at elevate temperature (EC3 2005b)

4.1.2.2. Formulation from Lie

Lie (1984) proposed different equations for the thermal properties of steel at elevated temperatures

Thermal capacity

$\rho_a.c_a = (0.004.\,\theta_a - 3.3).10^6$ (J/m^3 $^\circ$C)   for $0^\circ\,C < \theta_a \le 650^\circ\,C$

$\rho_a.c_a = (0.0068.\,\theta_a - 38.3).10^6$ (J/m^3 $^\circ$C)   for $650^\circ\,C < \theta_a \le 725^\circ\,C$

$\rho_a.c_a = (-0.086. \, \theta_a + 73.35) \cdot 10^6 \, (J/m^3 \, ^oC)$ for $725^oC < \theta_a \le 800^oC$

$\rho_a.c_a = 4.55 \cdot 10^6 \, (J/m^3 \, ^oC)$ for $\theta_a \ge 800^o \, C$

Thermal conductivity

The thermal conductivity of steel, λ_a is given by:

$\lambda_a = -0.022 * \theta_a + 48 \, (W/m^oC)$ for $0^o \, C < \theta_a \le 900^o \, C$

$\lambda_a = 28.2 \, (W/m^oC)$ for $\theta_a > 900^o \, C$

Thermal expansion coefficient (α_a)

$\alpha_a = (0.004 \cdot \theta_a + 12) \cdot 10^{-6} \, (m/m^o \, C)$ for $0^o \, C < \theta_a \le 1000^o \, C$

$\alpha_a = 16 \cdot 10^{-6} \, (m/m^o \, C)$ for $\theta_a \ge 1000^o \, C$

4.1.3 Stress strain curve for concrete at elevated temperatures (Eurocode)
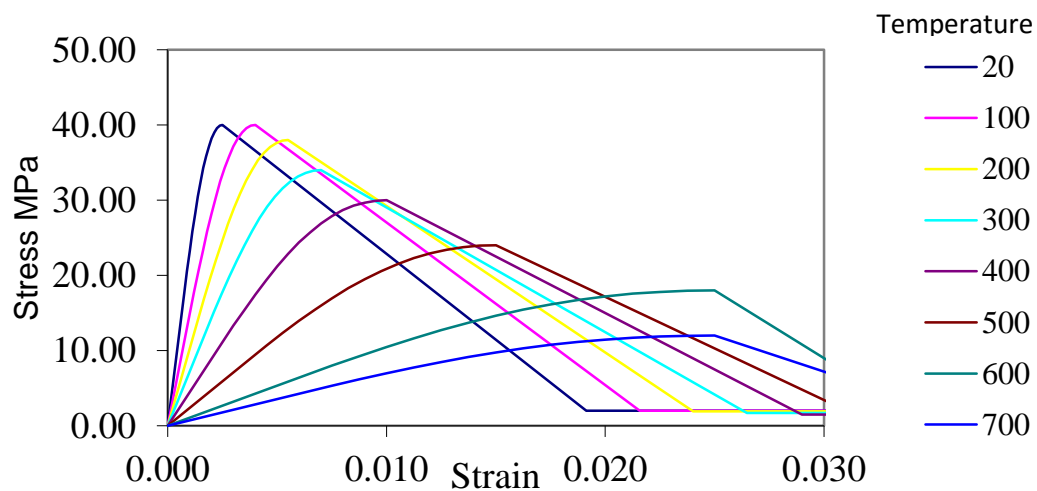
Figure 4.6. Shows the stress-strain curve of concrete (40 MPa)

4.1.4 Stress strain curve for steel at elevated temperatures (Eurocode)
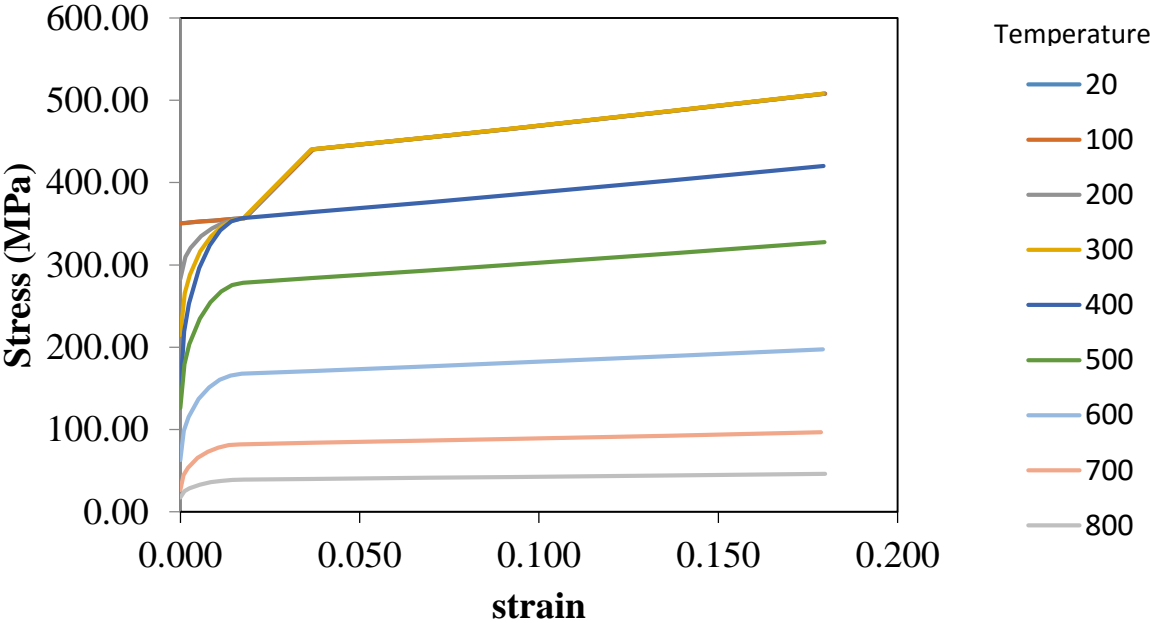
Figure 4.7. Shows the stress-strain curve of steel of strength (350 MPa)

4.2. Characteristics of the Numerical Model

A three-dimensional numerical model for simulating the fire behaviorr of CFT column was developed. The main parameters of the model were the length (L), steel tube thickness (t), external diameter (D), end conditions, and the material properties. The CFT column consists of three parts: the concrete core, steel tube and the loading plate. The loading plate was modelled as perfectly elastic and through this the applied load was transmitted to the concrete core and steel tube. The different parts which constitute the model are shown in fig 4.8.
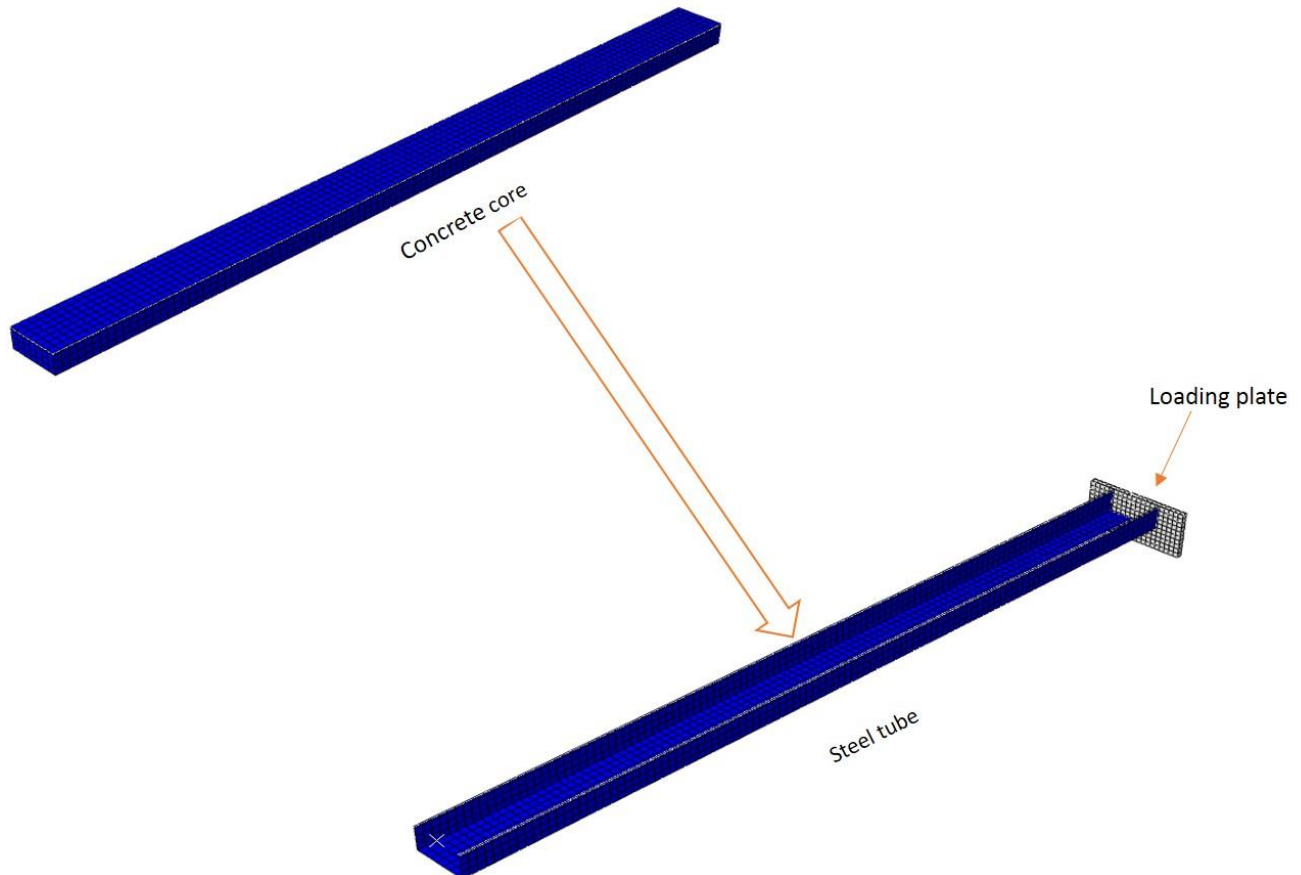
Figure 4.8. Different parts which compose the model

4.3. Scheme of analysis


```
┌──────────────────┐                    ┌──────────────────┐  Fire
│  1st Mode deformed│                    │  Thermal Model   │ ◄═══
│      Shape        │                    │                  │
└────────┬─────────┘                     └────────┬─────────┘
         │ Amplification                           │ Heat Transfer analysis
         ▼                                         ▼
┌──────────────────┐                    ┌──────────────────┐
│ Starting Geometry│                    │ Temperature Field│
└────────┬─────────┘                     └────────┬─────────┘
         │                                         │ Nodal T-t curve
         ▼                                         │
┌───────────────────────────────┐                 │
Axial load ═══►│      Mechanical Model      │◄────────┘
└──────────────┬────────────────┘
               │ Structural analysis    ┌──────────────────┐
               └──────────────────────► │ Structural response at│
                                        │ elevated Temperature  │
                                        └──────────────────┘
```
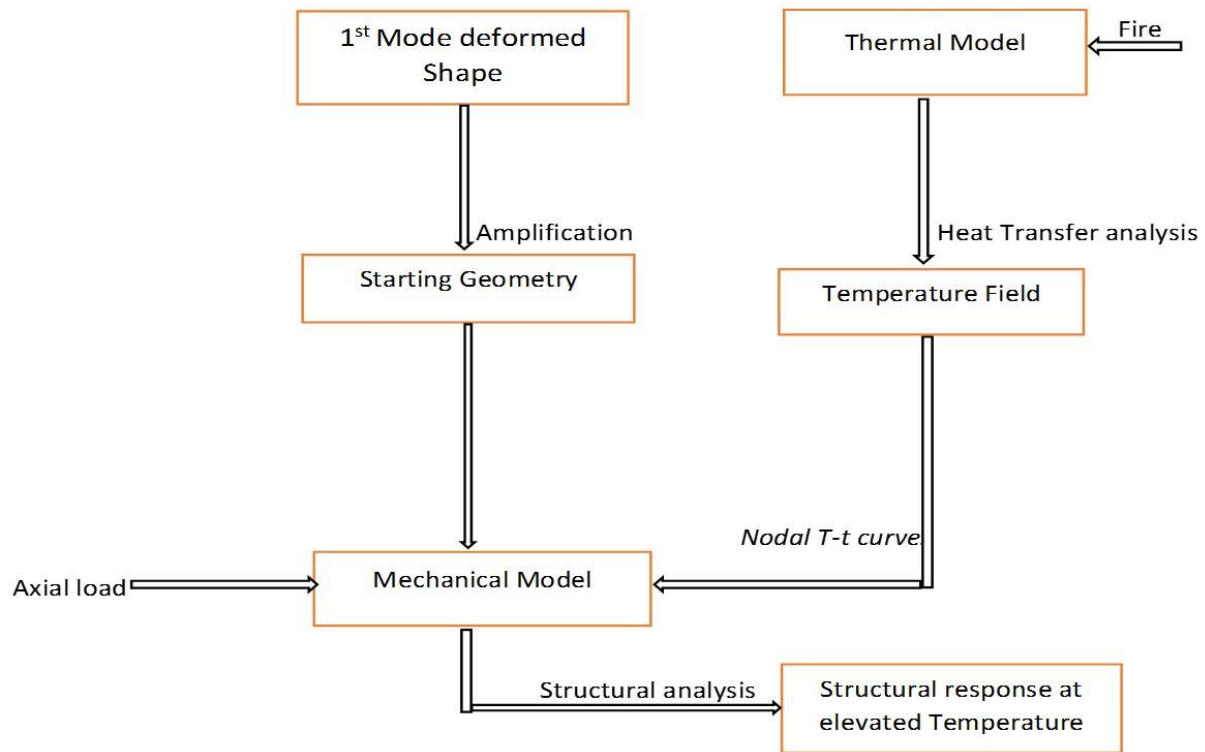
4.4. Analytical approach

A three-step sequentially coupled analytical approach was used to predict the thermal and structural behavior of CFT columns subjected to standard fire tests. The approach consists of three sequential analysis of steps, where the results from each step were used to continue the analysis in the subsequent step. The steps were as follows:

4.4.1. Step 1- Heat load

The thermal load (i.e, steel temperature) was given at the outer surface of the steel tube that is obtained from the experiments.

4.4.2. Step 2- Heat transfer analysis

The surface T-t curves determined in the step 1 were used as the thermal loading for simulating the heat transfer through the CFT cross-section and along the height. The heat transfer analysis was conducted using ABAQUS, which is commercially available nonlinear finite element analysis program. It simulates the heat transfer using the finite element formulation of first variation of basic energy balance equation along with Fourier law of heat conduction. The material thermal properties required for conducting the heat transfer analysis include thermal conductivity, specific heat for both the steel and concrete which are temperature dependent. The thermal material properties are taken from the Lie (1996) or Eurocode (1994-1-2). During the experiments a small vent hole was provided in steel tube at top and bottom to escape the pore water present in the concrete core. No heat loss was assumed at steel-concrete boundary i.e, temperature of steel and concrete were assumed as equal at boundary. The results from heat transfer analysis include nodal T-t curves for all the nodes of 3D finite element models.

4.4.3. Step 3-Stress analysis

The nonlinear stress analysis was conducted to determine the structural response of the column subjected to axial and the thermal loading. For conducting stress analysis we need the initial geometric imperfection of the column and the nodal T-t curves that are obtained in the step2.

Initial geometric imperfection

The initial geometric imperfection was simulated in the column as the first buckling mode shape of the column multiplied by an amplification factor. For this purpose eigen value analysis was conducted over a column subjected to axial loading. After obtaining the initial shape of the column it is imported into the mechanical model as the starting geometry to run the analysis. An amplification factor value of L/1000 or L/1500 (as specified by researchers) was then applied along the length in the stress analysis.

Thermal stress analysis

In this analysis, the mesh size in the model was kept same as that in the heat transfer analysis model. The initial imperfection geometric amplitude was then applied taking the amplification scale factor of L/1500 (or specified by researchers). In the first step axial load was applied at the top. During this step the column undergoes some deformation. In the second step, the heat (Nodal T-t curves) was introduced into the model while the axial load is maintained. The heating period is kept equal to the heat transfer analysis period. During the analysis the strength of the column decreases gradually and reaches a point where it cannot sustain any load. The time required to reach such condition where the column fails by compression or buckling is called as the *Fire Resistance time*.

4.5. Finite Element Modelling

Finite element based numerical simulations are used to model the behavior of CFT columns. Sequentially coupled thermal-stress analysis on 3-D models of CFT columns is performed to estimate (1) the temperature field and (2) the pre and post-failure structural behavior of CFT columns. If structural and thermal properties of steel and concrete are reported in the studies that report the CFT

column tests, these values are used. Otherwise, the values provided by the Eurocode (1994-1-2) are used.

For heat transfer analysis, only conduction part of the heat transfer was modeled. Steel temperatures as reported in the experimental studies were directly assigned to the outer surface of the steel tube in the numerical models. Steel tube was modeled using heat transfer plate elements with 5 or more temperature degrees of freedom along the thickness of the plate (DS4). The concrete core was modeled using 3-D linear heat transfer elements (DC3D8). For some of the tests simulated in this study, measured thermal and structural properties of steel and concrete were reported. For other tests, the properties available in the Eurocode [1994-1-2] were used. The interface between steel and concrete parts is assumed to offer no thermal inertia or resistance to the heat flow. This is a simplifying assumption. This will be rectified in the subsequent iterations.

For the purpose of the stress analysis, steel tube is modeled using 4-noded shell elements and concrete core is modeled using 8-noded solid elements. Concrete and steel are modeled as C3D8R and S4R elements respectively. Material properties (i.e., temperature dependent stress-strain curves and thermal expansion coefficients) for steel and concrete are taken from the Eurocode if the measured values are not available. Nodes at each column-end are rigidly connected to a representative point so that overall movement and rotation of the cross-section is allowed but relative displacements in the out-of-plane direction are prohibited. The interface between the concrete and steel parts was modeled as a hard contact with zero bond strength.

Chapter 5

Validation of Numerical Models

5.1. Validation for columns at ambient temperature

Circular columns:

M.L Romero and J.M Portoles (2011) conducted experiments to determine the capacity of Circular CFT columns at ambient temperature with eccentric loading. The following table gives the properties of the test specimens. The specimens are eccentrically loaded and their length are 2135 mm and 3135 mm respectively. Table 5.1 reports the details of the tested circular CFT column.

Table 5.1. Test properties and results of circular columns (M.L. Romero 2011)

Specimen	Diameter (mm)	t (mm)	L (mm)	e (mm)	f_y (MPa)	f_{ck} (MPa)	$N_{u,exp}$ (kN)	$N_{u,predicted}$ (kN)	
C1	100	3	2135	20	322	32.70	181.56	198	1.09
C2	100	3	2135	50	322	34.50	117.49	127.5	1.08
C4	100	3	2135	50	322	71.64	151.59	156.8	1.02
C6	100	3	2135	50	322	93.01	154.24	164.8	1.06
C30	125	5	3135	20	322	87.98	474.17	492	1.03
C31	125	5	3135	50	322	96.67	317.9	331	1.04

| C32 | 125 | 5 | 3135 | 20 | 322 | 107.33 | 489.47 | 530 | 1.08 |

S, Mises
SNEG, (fraction = -1.0)
(Avg: 75%)
+4.292e+02
+3.935e+02
+3.578e+02
+3.222e+02
+2.865e+02
+2.508e+02
+2.152e+02
+1.795e+02
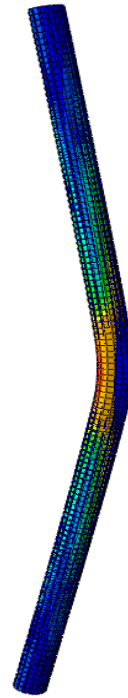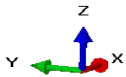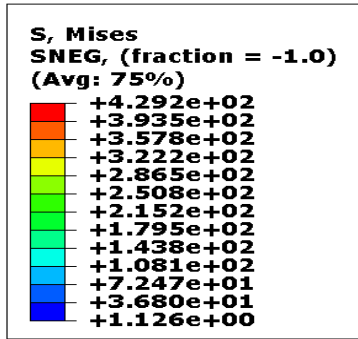+1.438e+02
+1.081e+02
+7.247e+01
+3.680e+01
+1.126e+00

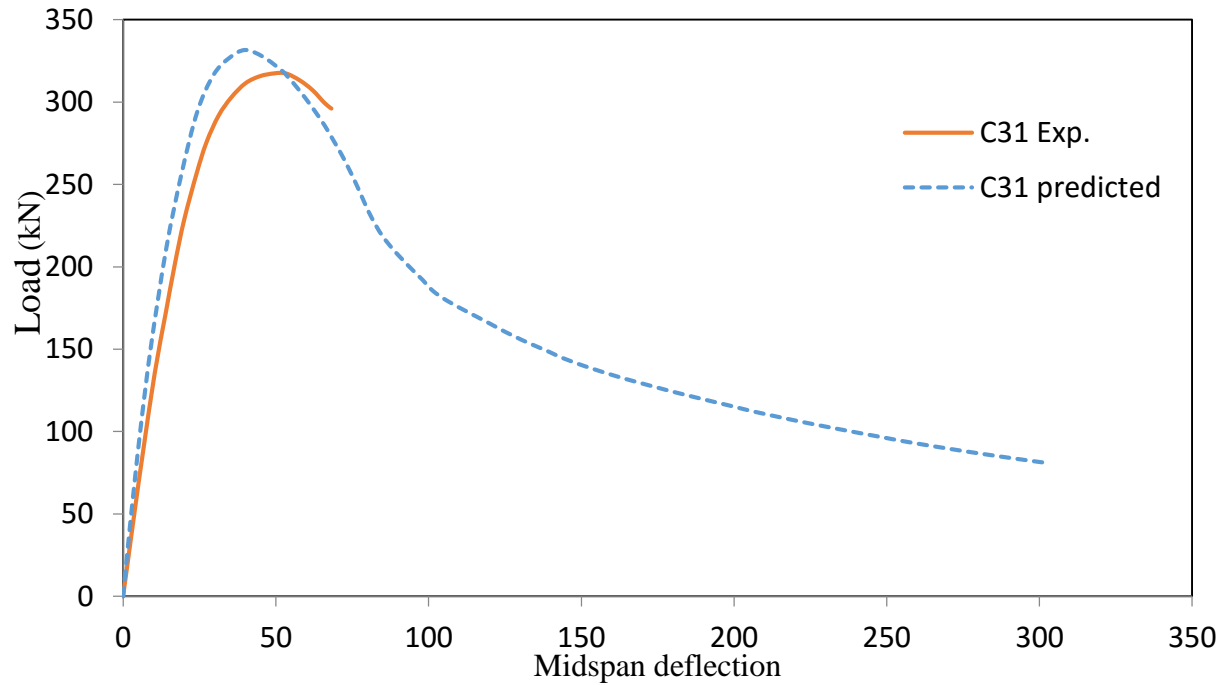Figure 5.1. Deformed shape of column C30

Figure 5.2. Load vs Mid-span deflection of column C31

Fig 5.2. Represents the axial load vs mid span deflection of the column C31 at the mid height. The failure load of the column predicted through FE analysis is 331 kN. But the failure load through the experiment is 318 kN. Although the trend is same the predicted load more by 4%.
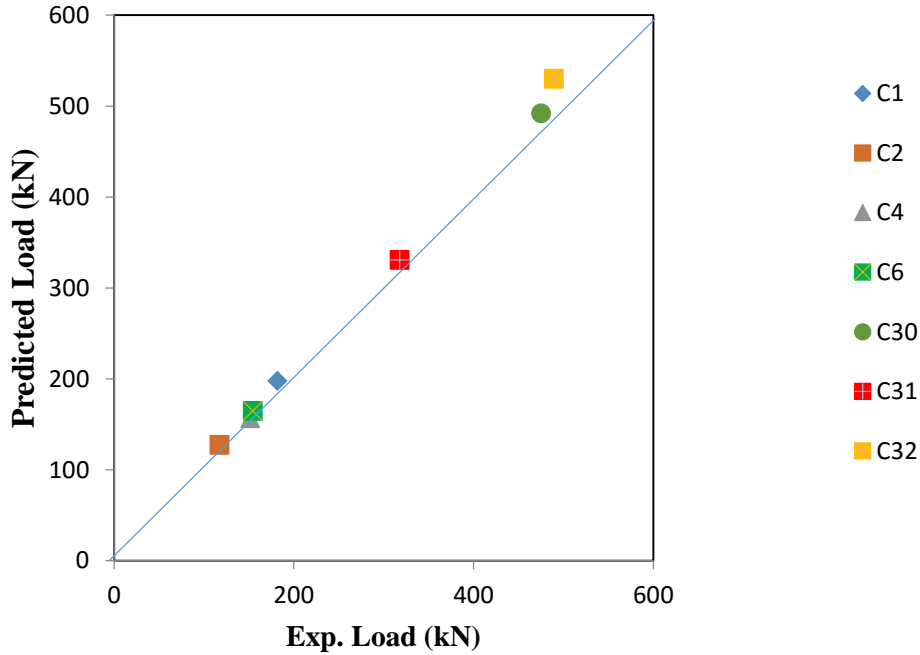
Figure 5.3. Comparison of predicted loads vs experimental loads of circular CFT columns tested

by Romero (2011) at ambient temperature

5.2. Validation for the columns exposed to fire

5.2.1. Assuming a perfect bond between steel and concrete so that the ends remain rigid:

The three dimensional numerical model was developed assuming a perfect bond and rigid at the ends. The column specimens used in this validation were tested by Han et. al (2003) at Tianjin, China. The tests were carried out by exposing the columns to heat in a furnace specially built for testing loaded columns. The ambient temperature at the start of the test was about 20°C. The length of the columns was 3810 mm. The boundary conditions employed for these specimens are fixed-fixed. The summary about these columns are presented in the given table.

Table 5.2. List of CFT columns analyzed from literature (Han et. al 2003)

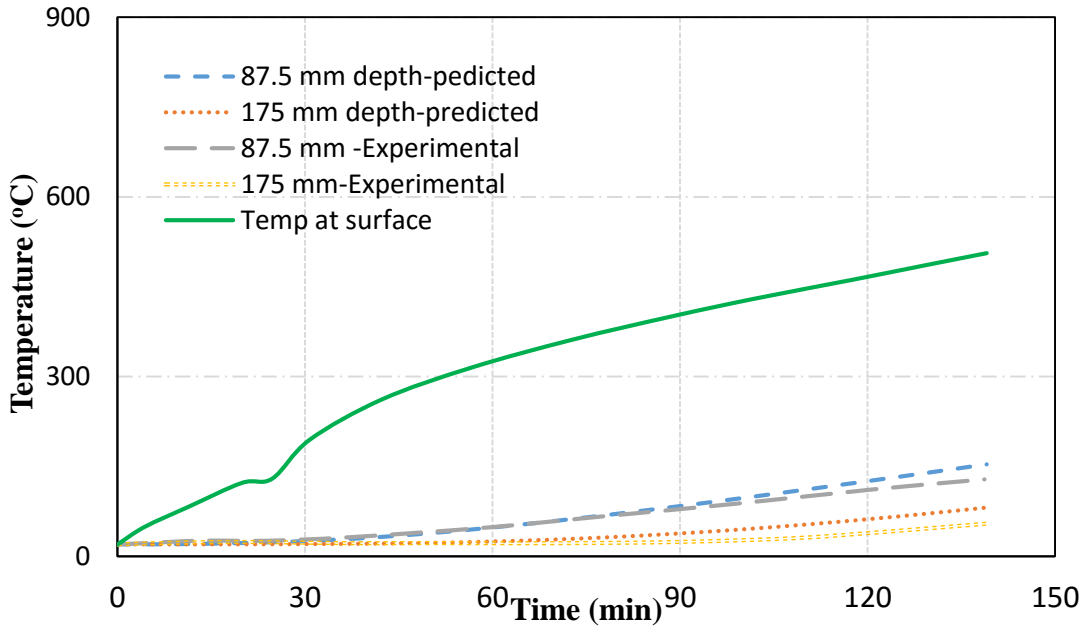| Specimen number	Sectional dimension (mm)	Boundary condition	f_y (MPa)	E_s ($*10^5$) (MPa)	f_{cu} (MPa)	a (mm)	Test load (kN)	e/r	R_{test} (min)	$R_{predicted}$ (min)
SP-2	350*350*7.70	F-F	284	1.83	18.7	11	2700	0	140	109
SP-3	350×350*7.70	F-F	284	1.83	18.7	7	1670	0.3	109	93

Figure 5.4 Comparison between Experimental and predicted temperatures for column SP-2

Figure 5.4 shows the temperature variations at the 87.5mm and 175mm. The temperature was applied on the steel outer surface in heat transfer analysis and its accuracy is checked at the given depths with the experimental values. The predicted temperature field matches with the temperature filed observed during the experiment reasonably.
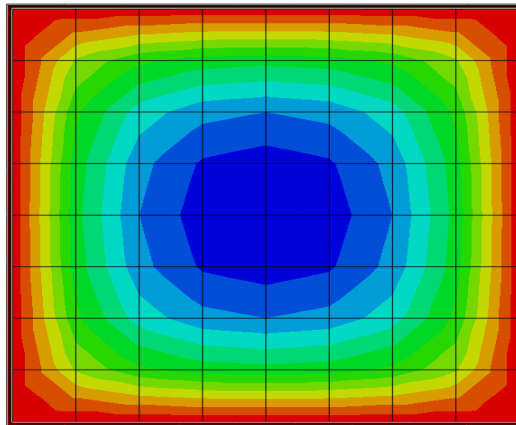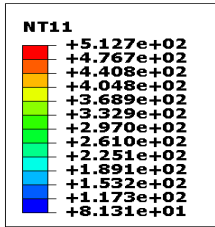
NT11
+5.127e+02
+4.767e+02
+4.408e+02
+4.048e+02
+3.689e+02
+3.329e+02
+2.970e+02
+2.610e+02
+2.251e+02
+1.891e+02
+1.532e+02
+1.173e+02
+8.131e+01

Figure 5.5. Temperature distribution in Column specimen SP-2

NT11
+5.900e+02
+5.463e+02
+5.026e+02
+4.589e+02
+4.151e+02
+3.714e+02
+3.277e+02
+2.840e+02
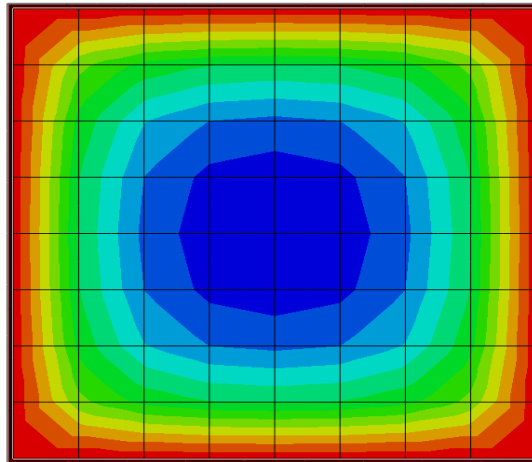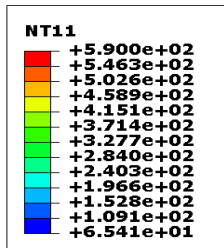+2.403e+02
+1.966e+02
+1.528e+02
+1.091e+02
+6.541e+01

Figure 5.6. Temperature distribution in Column specimen SP-3

Figures 5.5 and 5.6 show the temperature distribution in the columns after heat transfer analysis.
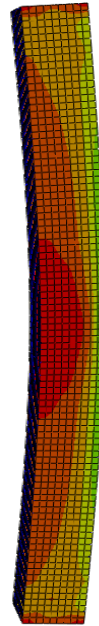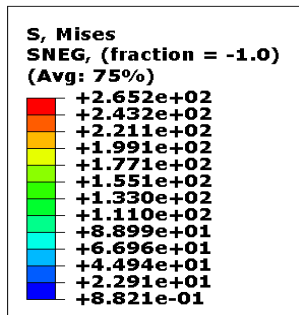
Figure 5.7. Stress distribution and the deformed shaped of column SP-2
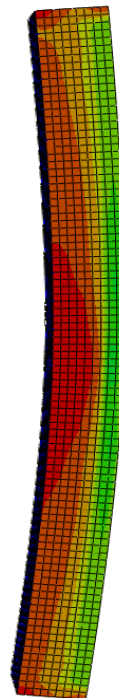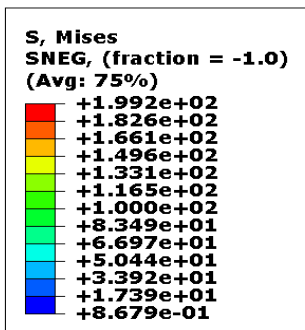
Figure 5.8. Stress distribution and the deformed shaped of column SP-3

Figures 5.7 and 5.8 show the stress distribution in the column at the onset of failure.
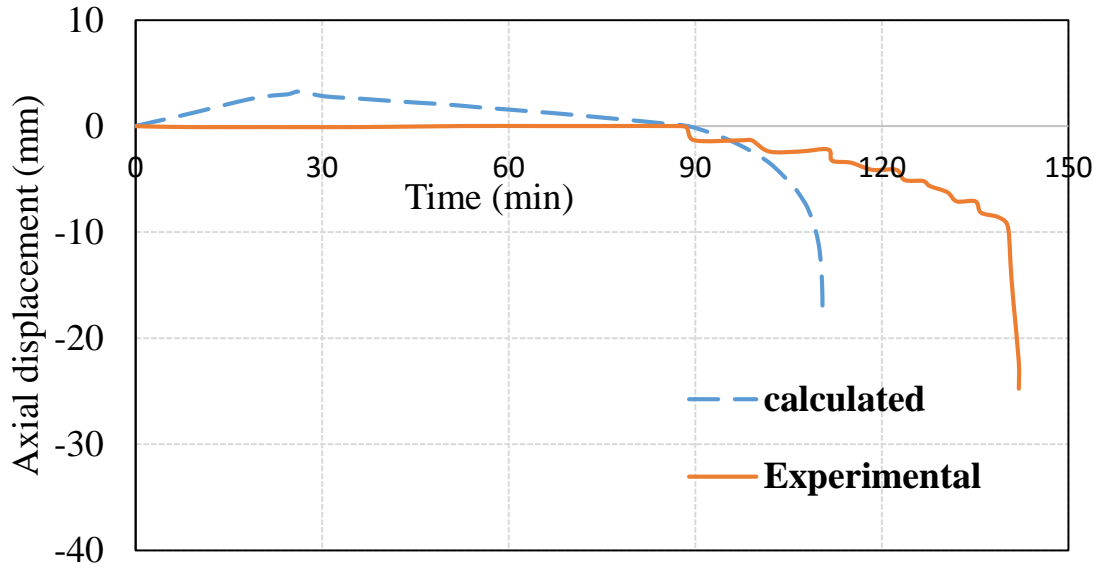
Figure 5.9. Comparison of measured and predicted axial displacement of column SP-2
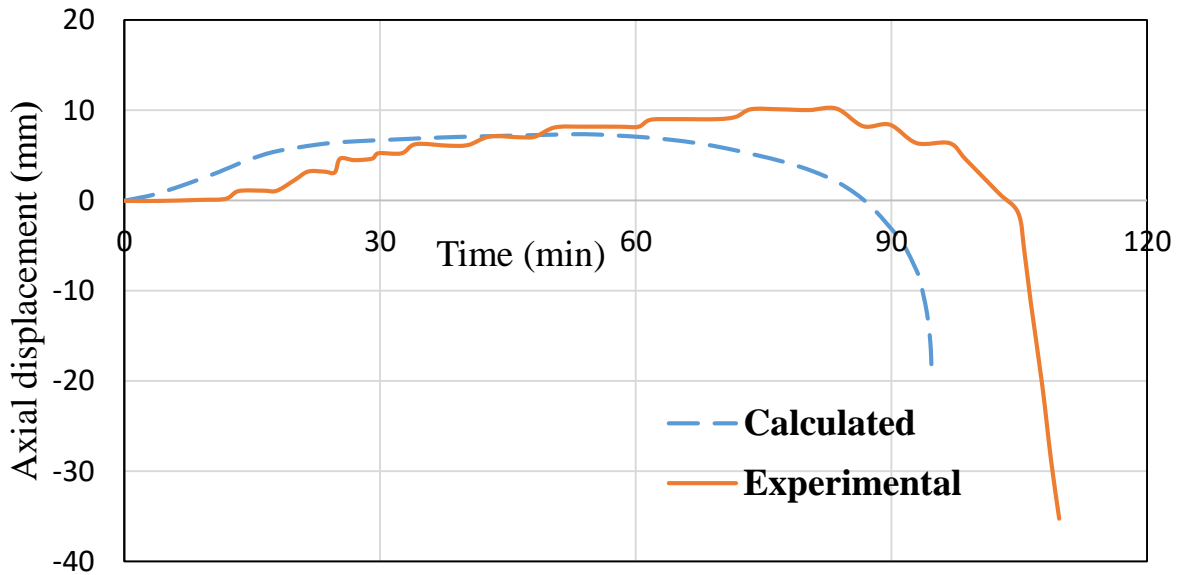
Figure 5.10. Comparison of measured and predicted axial displacement of column SP-3

Figures 5.9 and 5.10 shows the axial displacement variation with time for both columns. The predicted values are validated against the experimental results. The curve rise in the beginning and falls sharply after reaching certain period which describes its failure. The predicted capacity

35

of bot columns less than the fire resistance observed during the experiment. It is probably due to the way steel-concrete interface has been modeled. The interface between the steel tube and the concrete core assumes a perfect bond. Also, the ends are assumed to remain plane. As the steel tube is subjected to elevated temperatures, the steel tube wants to expands more than concrete core. As a result, concrete core is subjected to tensile forces. As concrete has little strength in tension, it immediately cracks thereby reducing the overall column strength.

Lie and Chabot (1992) also tested a number of CFT columns at elevated temperature one of these column SQ-20 is modeled using the technique described in above paragraphs. The predicted time vs vertical displacement plot is compared with the experimental data in figure 5.11.The details of column SQ-20 are presented in table 5.3.
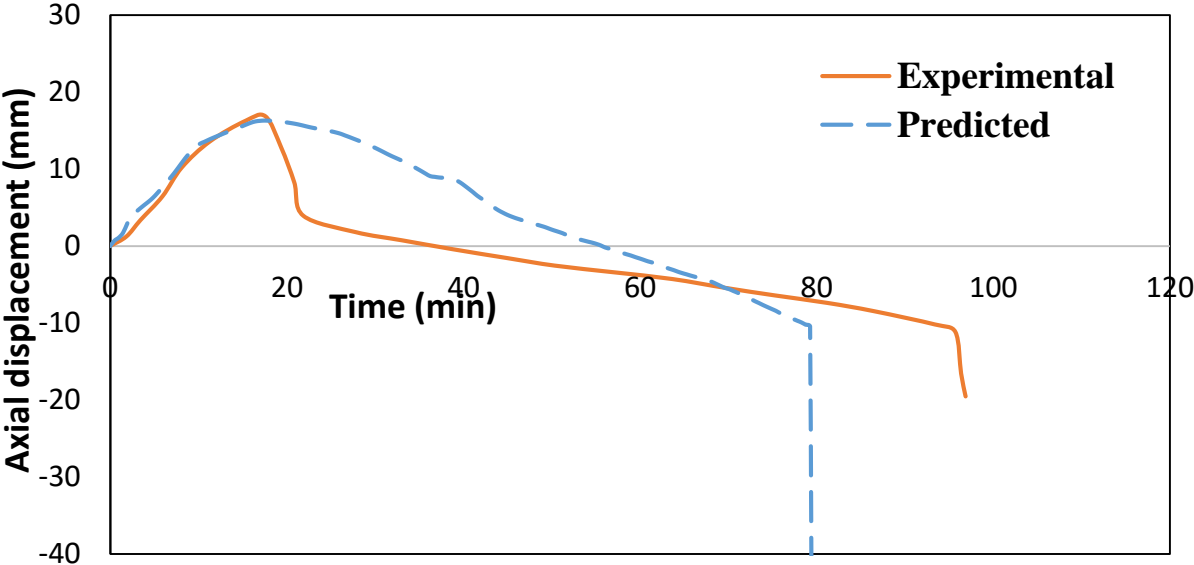

Figure 5.11. Axial displacement vs Time of column SQ20 (Lie and Chabot,1992) modeled

assuming rigid planes at the ends

5.2.2. Relaxing the bond between steel and concrete and the rigidity at the ends

The three dimensional numerical model was validated with the tests available from the experimental tests conducted by Lie & Chabot (1992). These tests were carried out in National Fire laboratory of the institute for research in construction, National research council of Canada. A number of square CFT columns were tested with fixed-fixed boundary condition and without any external fire proofing agent. The length of each column that was tested is of 3810 mm. The concrete used in the column is of siliceous aggregate. CFT columns were heated in the middle 3048 mm of length. The room temperature before the start of the test is kept at 20°C. The concrete used in the column is of siliceous aggregate. During the test, the column was exposed to heating in such a way that the average temperature in the furnace as closely as possible ASTM – E119 standard temperature-time curve. The details of the column specimens are presented in table 5.3.

In numerical modeling, the steel-concrete interface is modeled as the hard contact with zero as bond strength. Axial load is applied on the plate fixed at the ends to the steel tube, which allows the steel plate to expand more than the concrete core and carry the entire load for first 15-30 minutes. Then the steel tube buckles locally and the loads gets transferred to the concrete. The deformed shapes of the numerical results resemble the experimental failure shapes of CFT column (Figure 5.13, 5.16, 5.19), where the local buckling of the steel surface is seen predominantly.

Figures 5.14, 5.17, 5.20 show the predicted behavior of column SQ-17, SQ-20, SQ-24. It can be observed that the models were able to predict the failure shapes and the failure times of all the columns with reasonable accuracy. Also, the shape of time vs vertical displacement plots are in good agreement with experiments.

Table 5.3. List of CFT columns analyzed from literature (Lie and Chabot 1992)

Column No.	Sectional dimension (mm)	Boundary condition	f_y (MPa)	E_s ($*10^5$) (MPa)	f_{cu} (MPa)	Test load (kN)	R_{test} (min)	$R_{predicted}$ (min)	Failure Mode
SQ-17	254*254*6.35	F-F	350	2	58.3	1096	62	62.2	C
SQ-20	254*254*6.35	F-F	350	2	46.5	931	97	88	C
SQ-24	304.8*304.8*6.35	F-F	350	2	58.8	1130	131	123	C

Column SQ-17
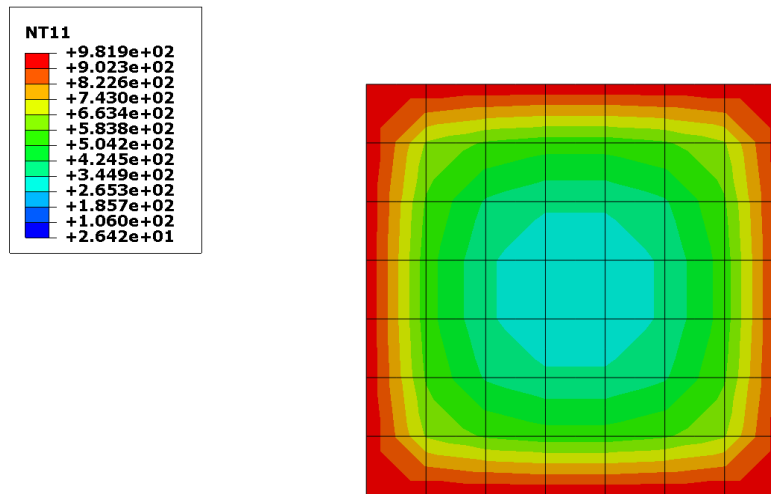
Figure 5.12. Temperature distribution in Column SQ17
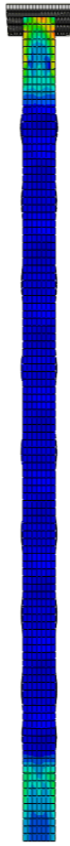
Figure 5.13. Deformed shapes of Column SQ-17

a) Just before failure b) At failure c) Experimental

Figure 5.14. Comparison of experimental and predicted axial displacement of column SQ-17

Column SQ-20

Figure 5.15. Temperature distribution in Column SQ20

Figure 5.16. Deformed shapes of Column SQ-20

a) Just before failure b) At failure c) Experimental
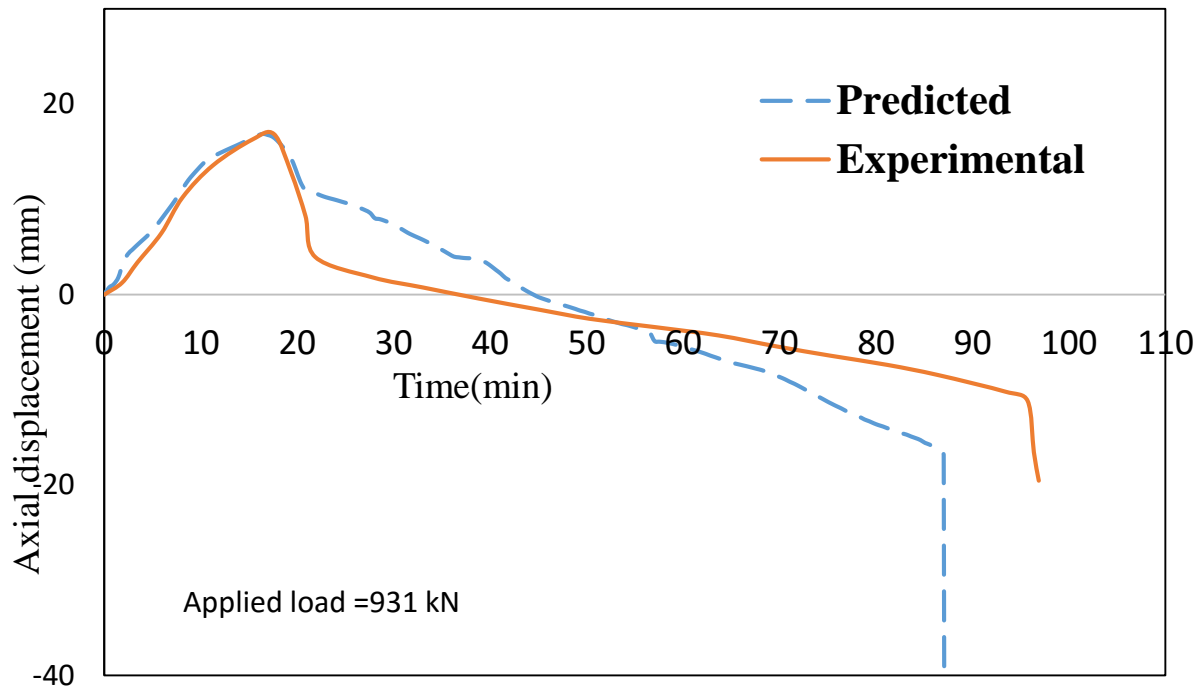
Figure 5.17. Comparison of experimental and predicted axial displacement of column SQ-20

Column SQ-24
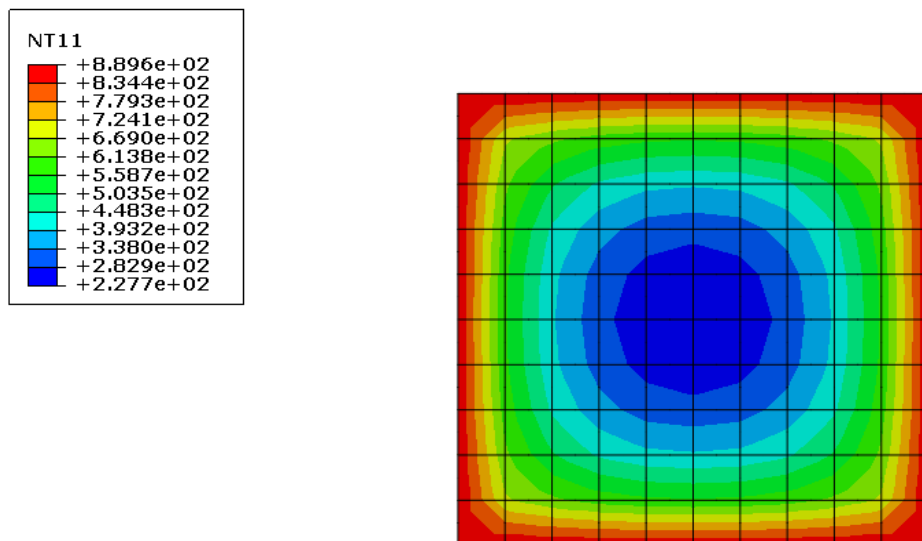
Figure 5.18. Temperature distribution in column SQ-24
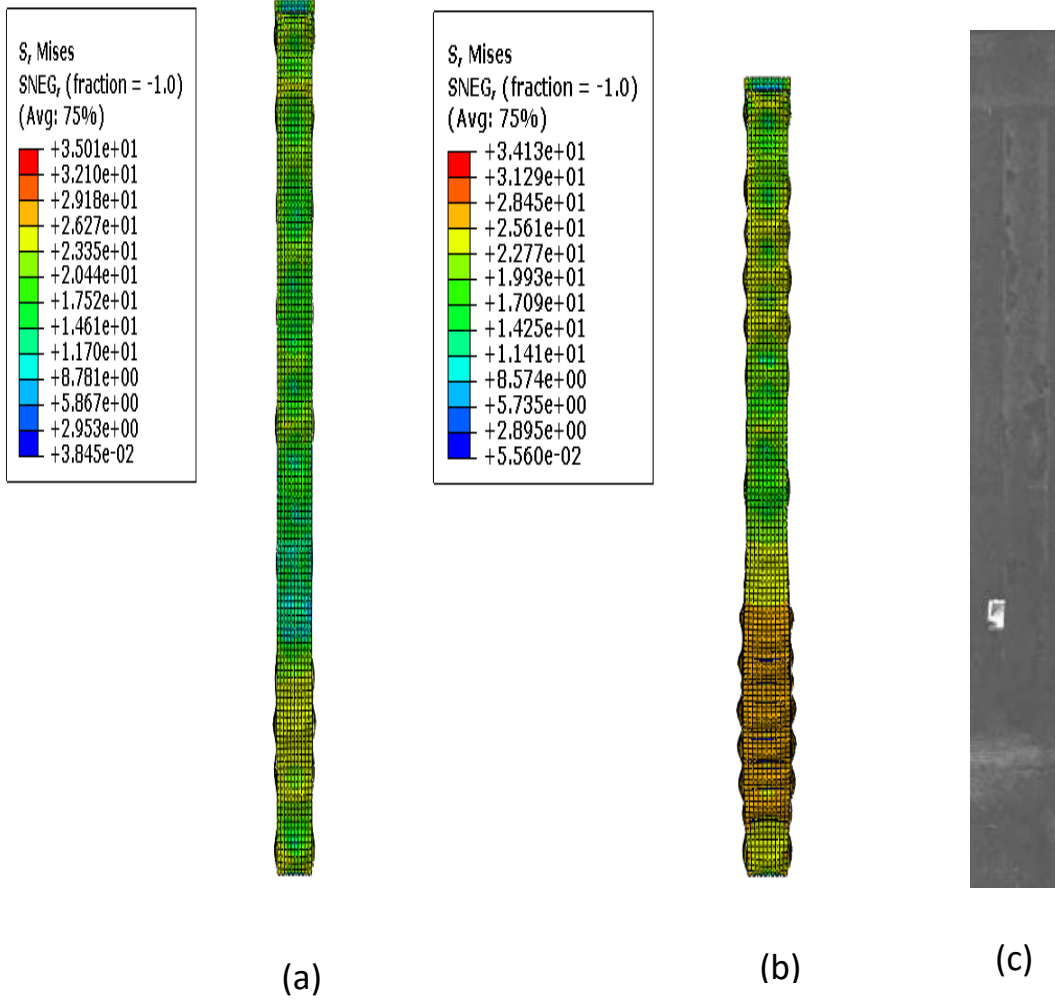
Figure 5.19. Deformed shapes of Column SQ-24
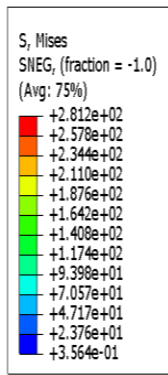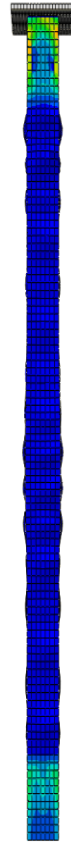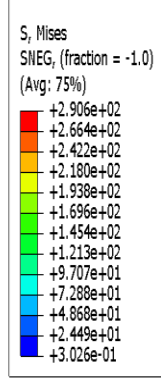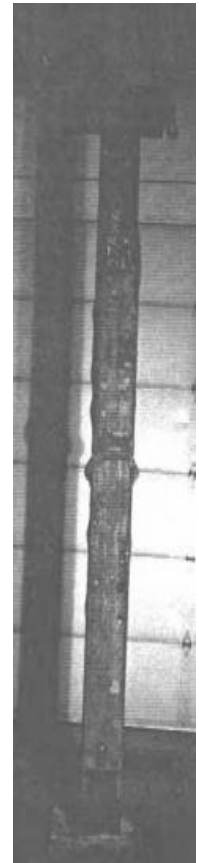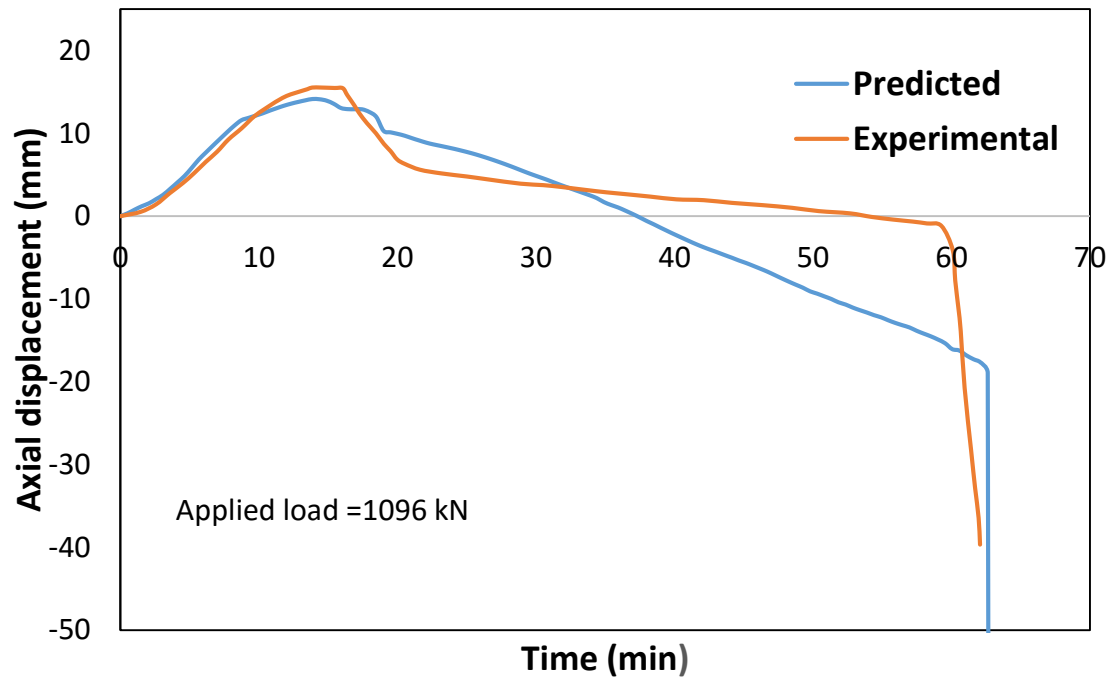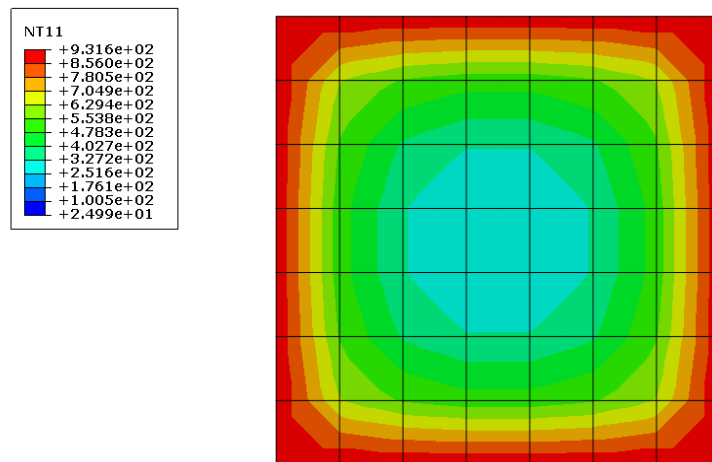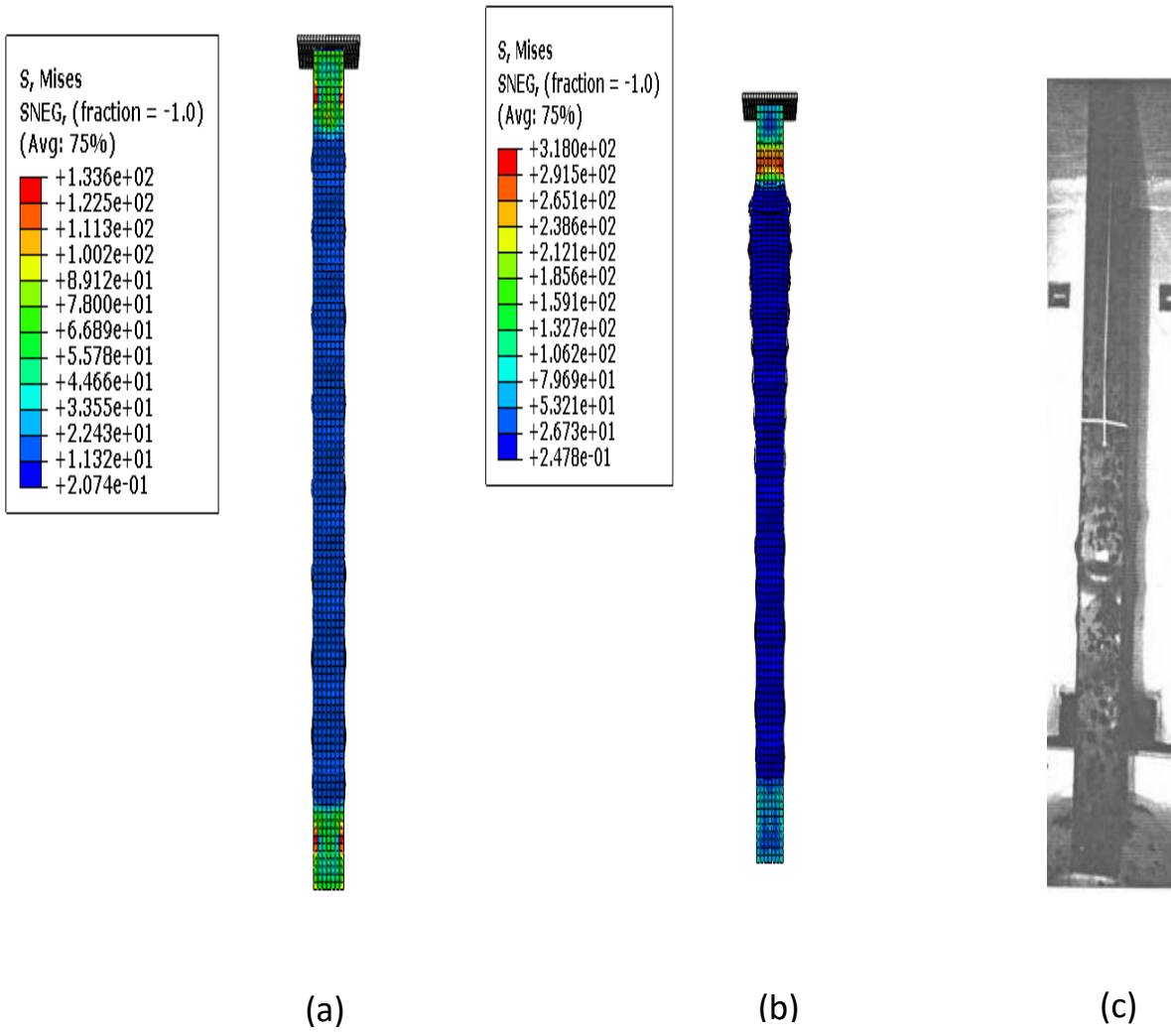
a) Just before failure b) At failure c) Experimental
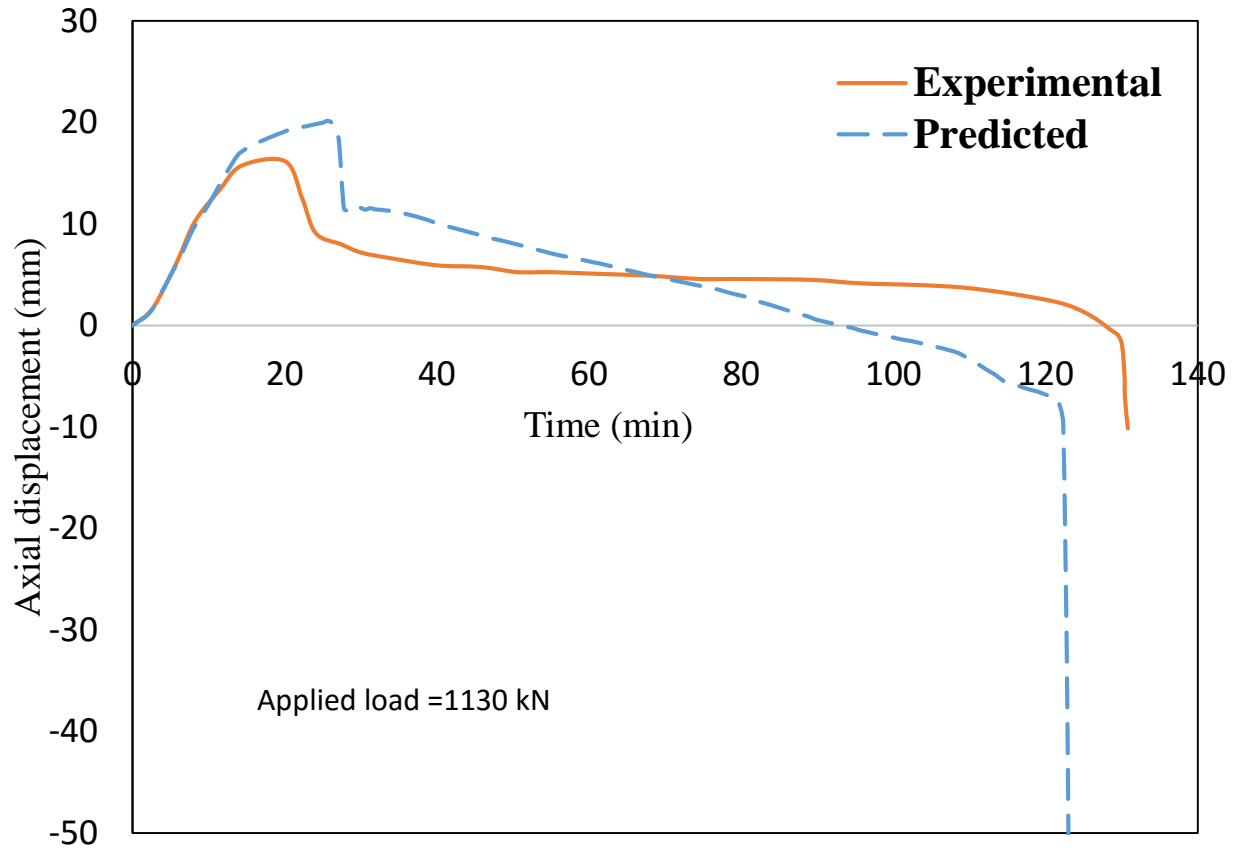
Figure 5.20. Comparison of Experimental and Predicted axial displacement of column SQ-24

Chapter 6

Sensitivity Study

It is important to understand how certain parameters, especially the ones about which there may be uncertainty while developing the numerical models, affect the overall structural behavior of the columns. The factors that are studied were initial geometric imperfection, steel concrete interface, friction coefficient between steel-concrete interface and concrete post crack tension properties. But the steel-concrete interface and concrete post-crack tensile properties were found to be of high importance in accurately modeling the compression behavior of CFT columns.

6.1 Initial Geometric imperfection:

Geometric imperfection affects the global buckling behavior of CFT columns. The geometric imperfection for the CFT columns were specified as the first buckling mode shape multiplied by an amplitude which defines the maximum geometric imperfection along the column length. Two different geometric imperfection (i) L/7500 and (ii) L/1500 are considered. The effects of the geometric imperfection on the fire resistance of CFT columns are studied and validated with the experimental results. The comparisons on the axial displacements with the experimental results are shown below:
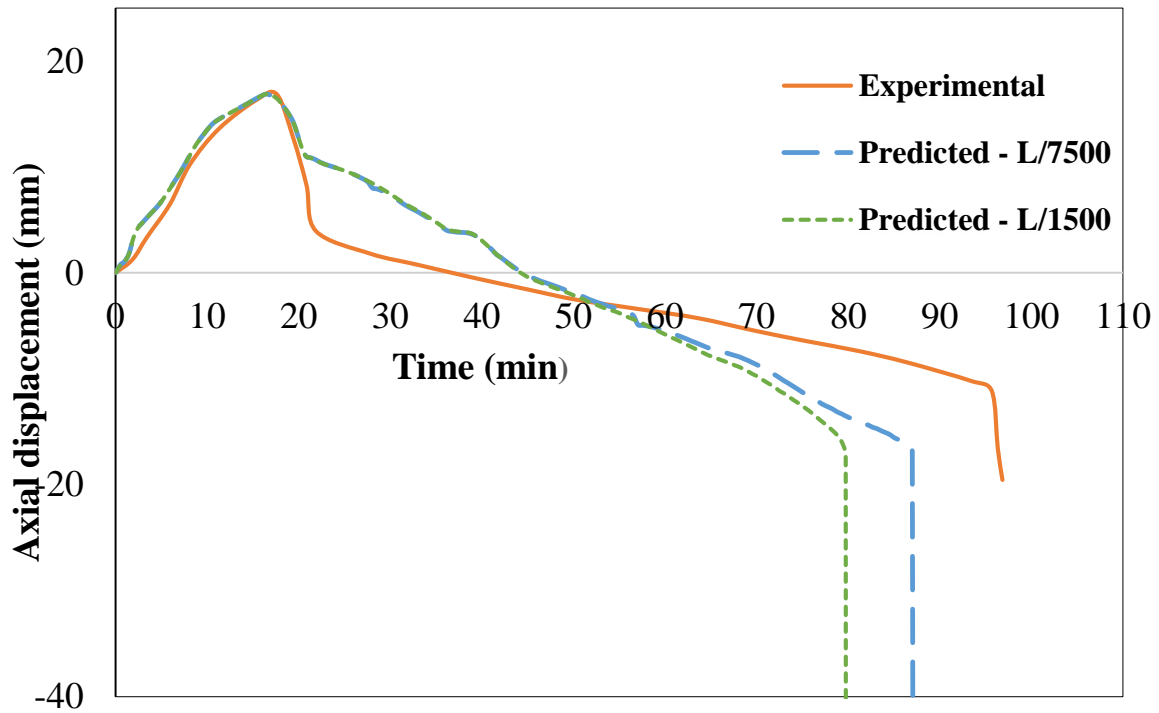
Fig 6.1. Comparison of the axial displacements of column SQ-20 with different imperfection

factors

The Experimental fire resistance of CFT column is 97 minutes. But the predicted fire resistance

of column with L/7500 and L/1500 as imperfection factors are 88 minutes and 80 minutes

respectively. The results shown a variation of 9% and 17% with the experimental results by

using these imperfection factors.
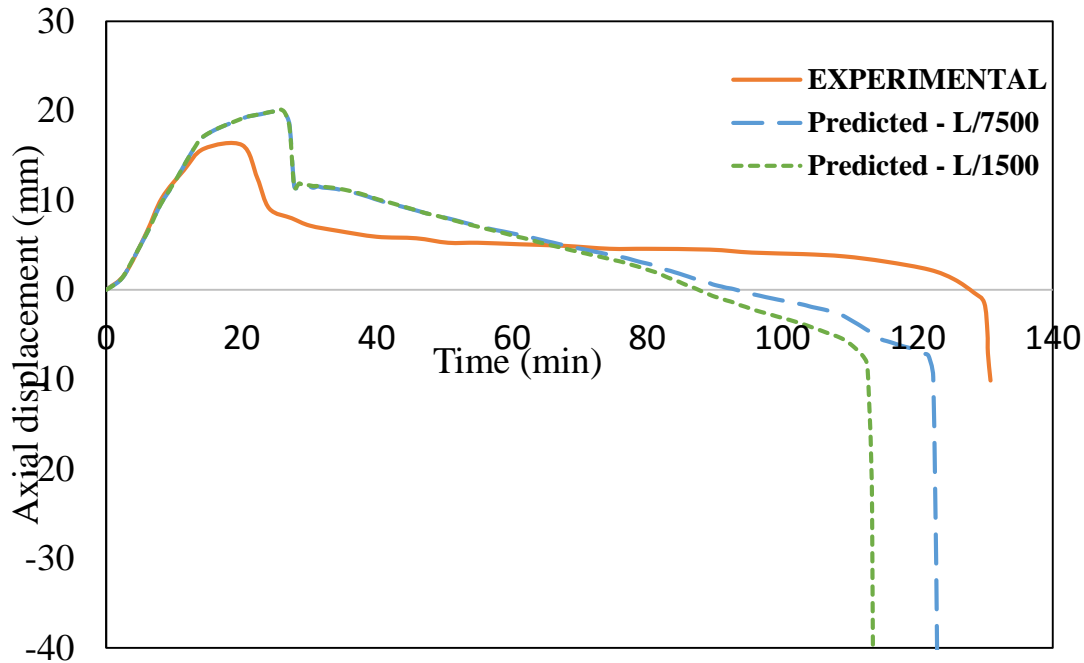
Fig 6.2. Comparison of the axial displacements of column SQ-24 with different imperfection

Factors

The Experimental fire resistance of CFT column is 131 minutes. But the predicted fire resistance of column with L/7500 and L/1500 as imperfection factors are 123 minutes and 114 minutes respectively. The results shown a variation of 6% and 13% with the experimental results by using these imperfection factors.

The comparisons of the experimental results with the analytical results indicate:-

(i)Increasing the imperfection amplitude reduces the fire resistance of CFT columns.

(ii)The initial geometric imperfection of L/7500 gives the better comparison with the experimental and the analytical results.

6.2. Steel-Concrete interface:

Modeling of Steel-concrete interface plays a vital role in the structural behavior of CFT columns. It is observed that the overall strength of CFT columns are sensitive to the interface behavior. Two extreme cases namely 1) Perfect bond between the steel and the concrete and steel interface 2) Hard contact with zero bond strength is considered in FEM simulations and the results are compared with the behavior of tested columns.

(a) Experimental   (b) Perfect bond   (c) hard contact
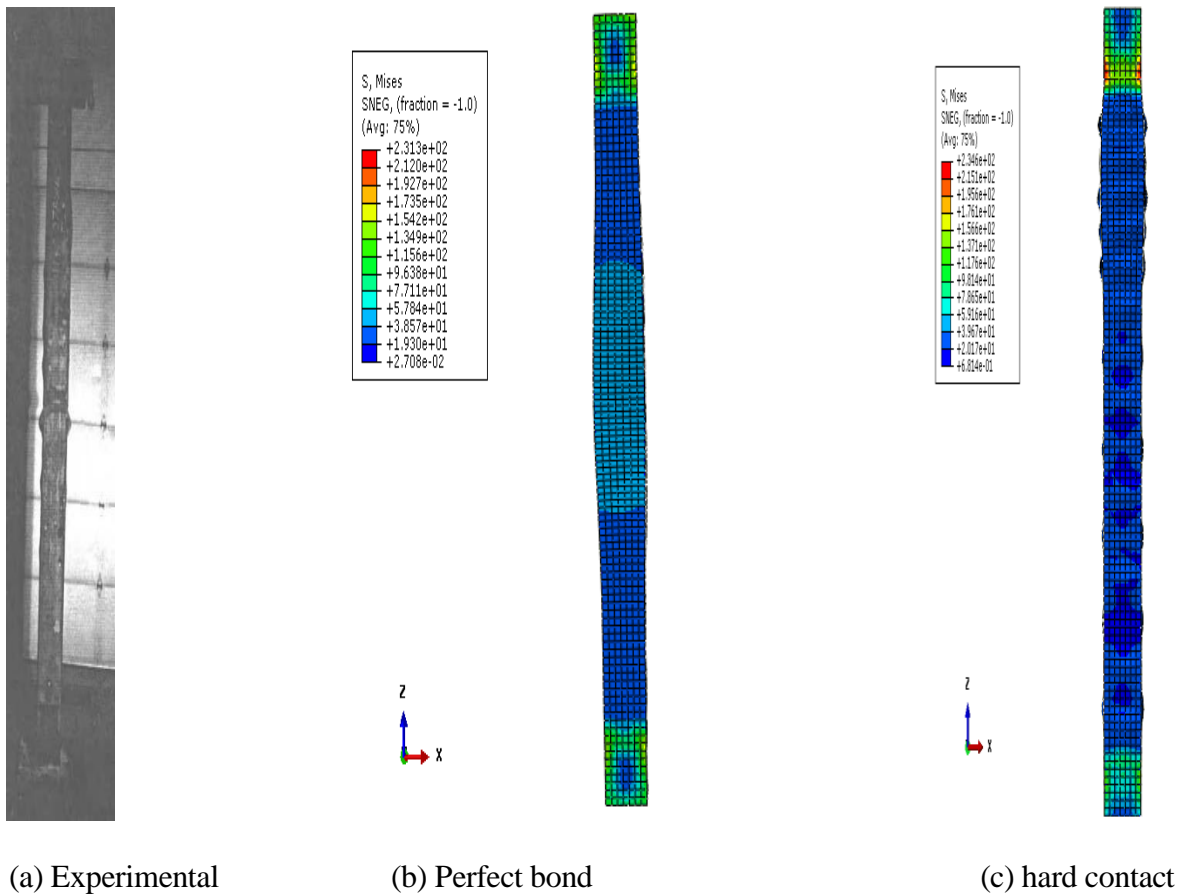
Figure 6.3. Deformed shapes of a column (a) Experimental and b) predicted with the assumption of a perfect bond and zero bond strength

Figure 6.3 compares the deformed shape of the column tested by Lie and Chabot (1992) under two interface assumptions i.e, full bond and hard contact. It is observed that the perfect bond doesn't allow the steel to buckle locally. The test specimen has undergone significant local buckling which is well captured by the simulation which has zero bond strength. On comparing the simulated fire resistance of CFT column it is revealed that the model with concrete interface as zero bond strength has predicted higher fire resistance than the model with steel and concrete interface as perfect bond. For example, column SQ17 is predicted to have a fire resistance of only 53 minutes if the interface is modeled as perfectly bonded. However, the predicted fire resistance increases to 62 minutes if the interface is modeled to have zero bond strength. Further investigation indicates that there is hoop stress induced by uneven expansion of the elements in the column cross section. Portions of the cross-section closer to the center are at a lower temperature than the surface. Therefore, internal elements (i.e., concrete core) expand less than the outer elements (i.e., steel tube). If the interface is modeled as perfect bond, this differential expansion leads to a tensile hoop-stress in the peripheral elements of the concrete and a compression hoop-stress arises in the steel tube. As concrete has very low strength in tension, this leads to cracking of the concrete core, which, in turn, leads to a reduction in the overall column capacity.

6.3. Concrete post-crack tension properties:

Post-cracking behavior of concrete in tension is found to have a significant amount of influence on the behavior of CFT columns at elevated temperatures. A simply supported circular CFT column (length =2135 mm, outer diameter = 100 mm, and steel tube thickness = 4 mm) was simulated to study the effects of change in post-crack behavior of concrete. These simulations were conducted in three different conditions, namely (i) ambient temperature, (ii) uniform temperature of 600 ^{o}C, and (iii) simulated thermal loading where steel temperature rises to 600 ^{o}C in approximately 20 minutes Two different post-cracking tension properties were considered. (i) Post cracking strength is reduced to 20% of the maximum tensile strength after a plastic tensile strain of 0.01 and (ii) concrete retains its full tensile strength for very large plastic strain. It was observed that for columns at ambient temperature, the two types of post-crack concrete behaviors leads to a very small difference (0.3%) in the column capacities. In the case where the column is at a uniform temperature of 600 ^{o}C, the difference between the column axial load capacities estimated using the two types of post-crack concrete behaviors was approximately 9.2%. However, for the column subjected to a non-uniform temperature distribution, the difference between the axial load capacities estimated using the two post-crack concrete behaviors was approximately 13.2%. This clearly indicates that at ambient temperature, concrete is hardly subjected to tension cracking; therefore, post- crack tension property of concrete does not have a significant effect on the column capacity. However, as the temperatures rise, due to uneven expansion of different elements, some portions of concrete may be subjected to tensile stresses. Therefore, accurate modeling of post-crack tension behavior of concrete behavior becomes very important.
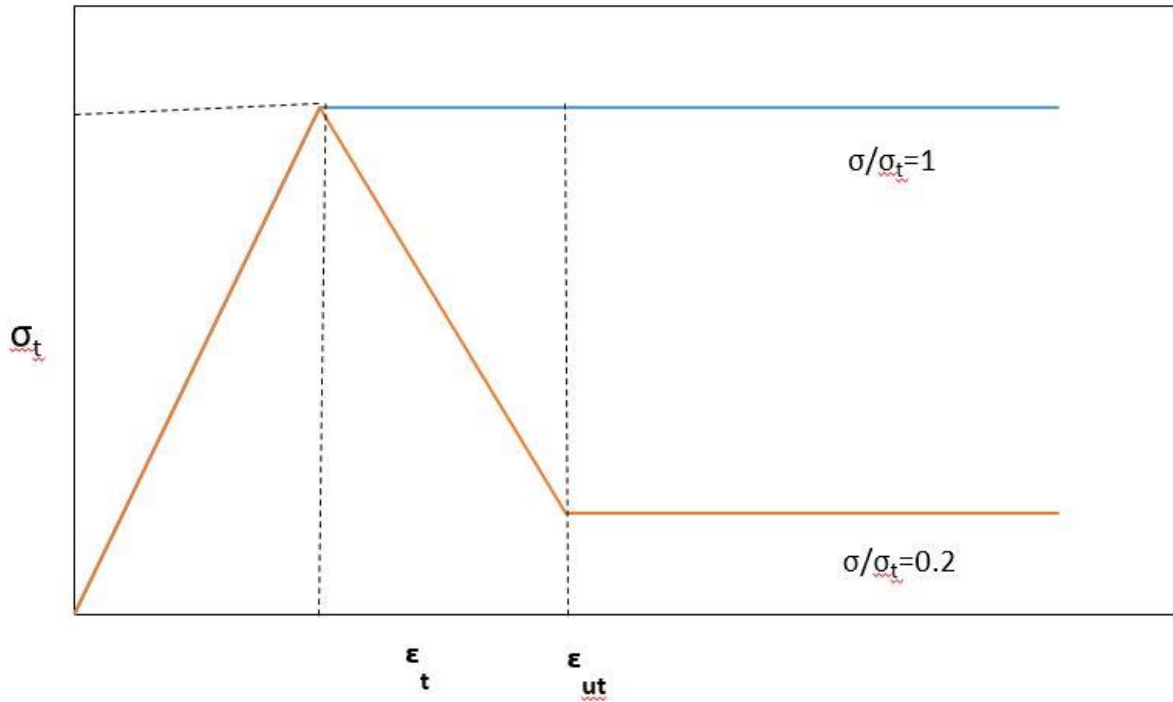
Figure 6.4. Concrete tension stiffening model
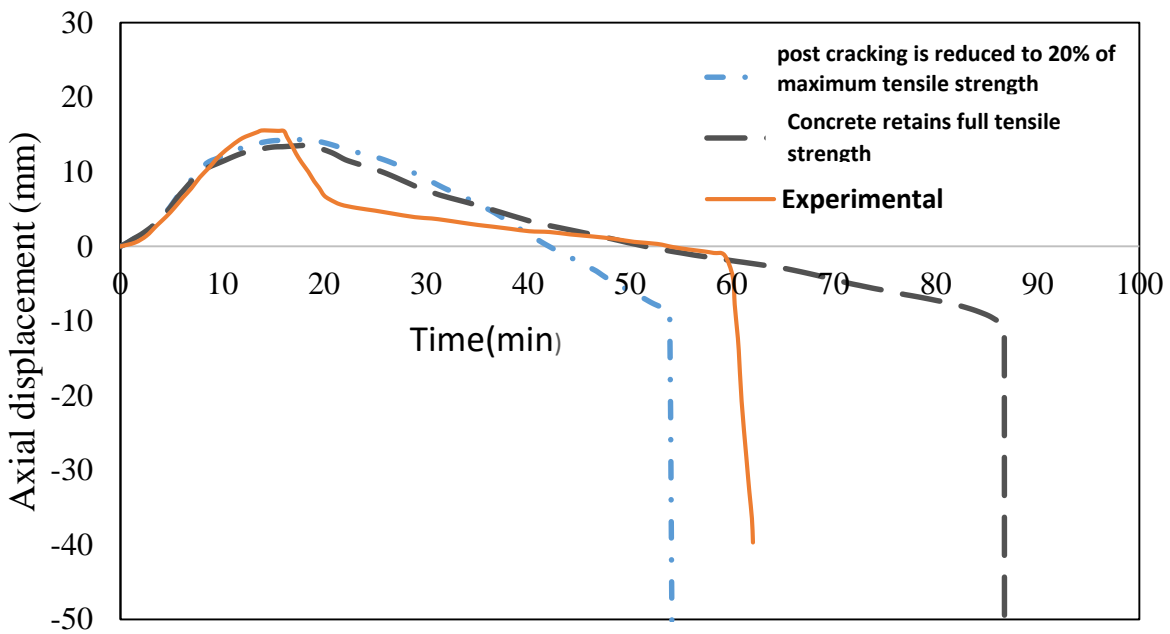
Fig 6.5. Comparison of axial displacements with respect to different post cracking tensile

Properties with perfect bond

51

6.4. Friction between the Steel-Concrete interface:

Effects of different values of coefficient of friction ranging from 0.3 to 0.8 are studied. No difference was observed in overall fire response. Thus, the friction coefficient between the steel and concrete surface doesn't have any influence on the column fire behavior. This is due to the fact that steel and concrete core slide relative to each other in fire situation, thus frictionless model can be adopted.
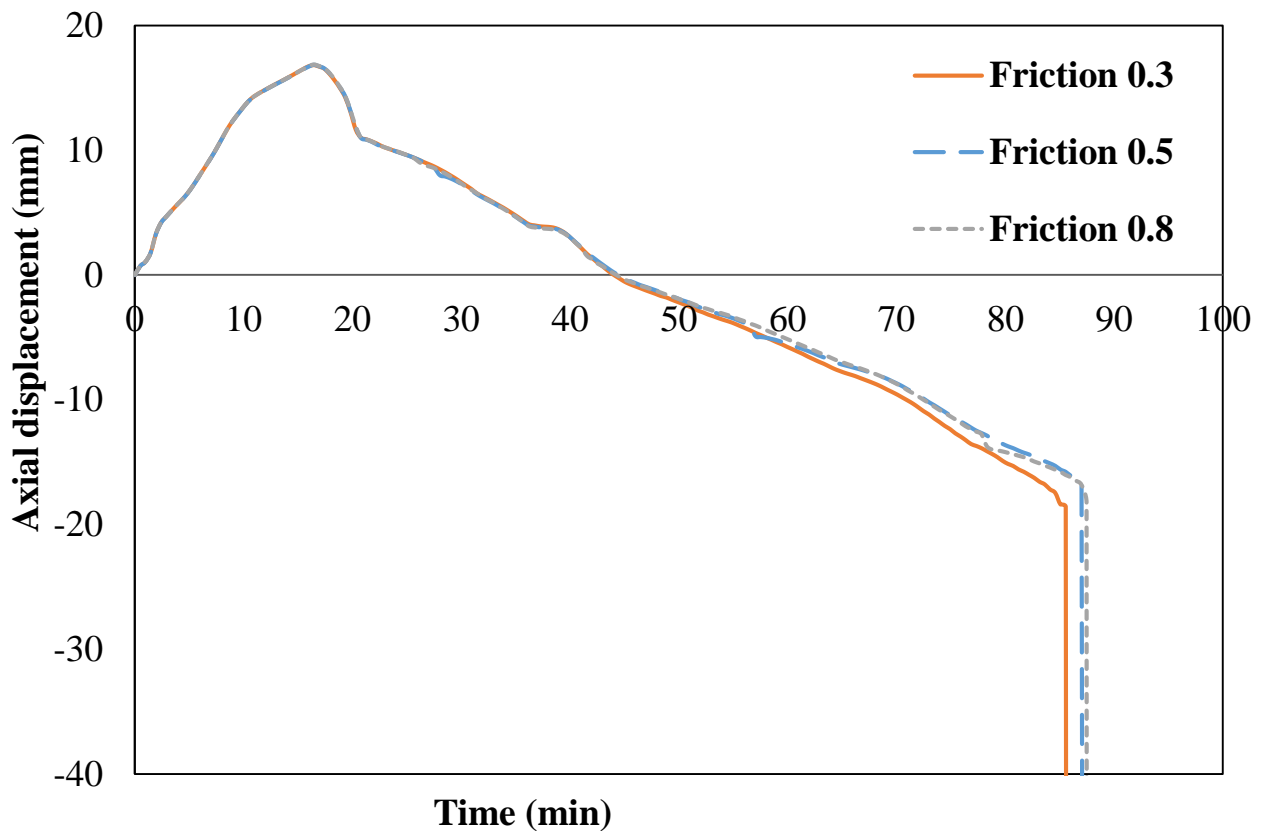
Figure 6.6. Comparison of axial displacements with different coefficient of friction

6.5. Behavior of CFT columns in fire and effect of end-plate:

At ambient temperature, the applied axial load is carried by both hollow steel section and the concrete core. When the column is exposed to fire, both the steel section and concrete core start to expand this is indicated by steep increase in axial deformation. During that stage the steel section carries all the applied load because it expands more rapidly than the concrete core. As the temperature increases, the steel loses its ability to support the load and the column suddenly contracts usually after 20-30 minutes. This is accompanied by bulging of steel section. The load is gradually transferred to concrete core, which loses strength more slowly than steel due to its lower thermal conductivity and higher heat capacity of the concrete. The column then progressively contracts as the temperature increases and ultimately fails by either buckling or compression, depending on the slenderness of the column. At the failure, the concrete core carries entire load.

Load is applied to CFT column through the loading plate. Loading plate is tied to the steel surface and the interface between steel and concrete is modelled as hard contact with zero bond strength. During the first stage, i.e, application of axial load, the CFT column goes into compression to resist the applied axial load. But when the heat was applied in the second stage the steel tube expands and carries the load alone. As the temperature increases the steel tube deforms and slowly the load gets transferred from steel to concrete.

The figures 6.7 to 6.9 shows the behavior of the CFT column during fire. Figure 6.10 shows the comparison of axial displacement vs time with two different assumptions.
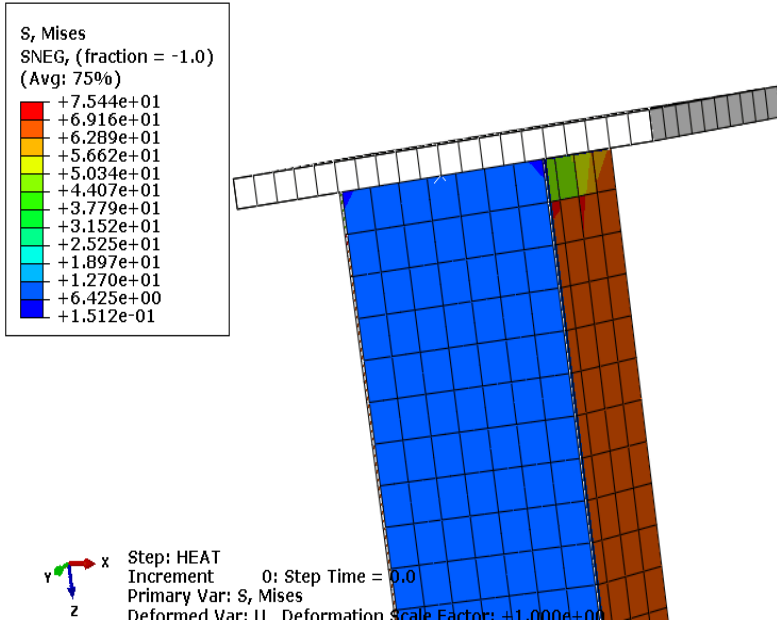
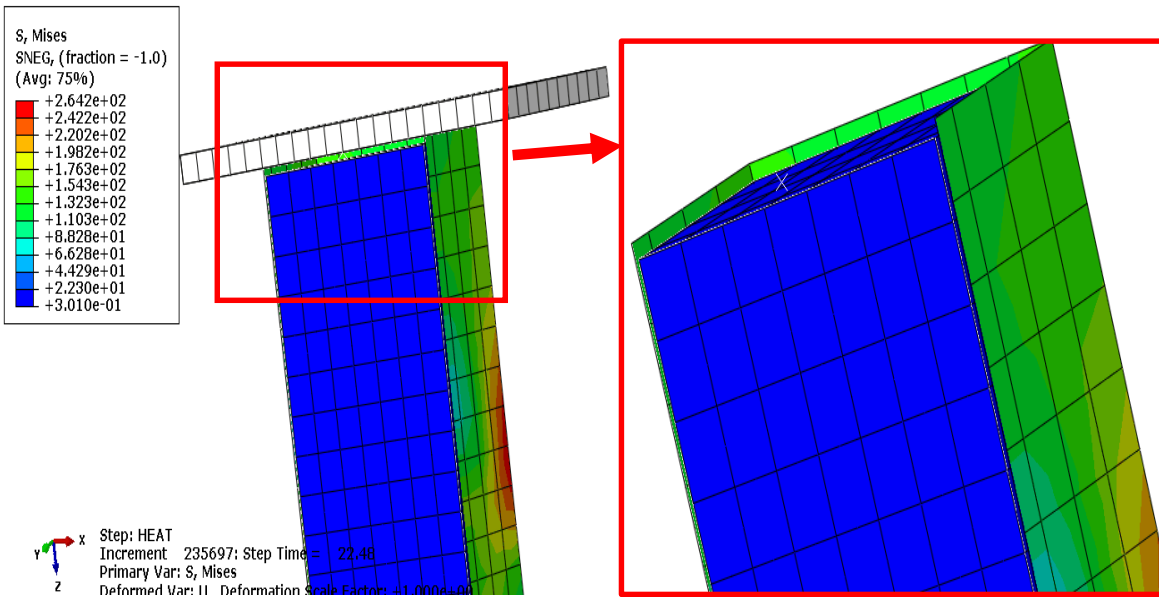Figure 6.7. CFT column before subjected to heat

Figure 6.8. CFT column during expansion of steel tube
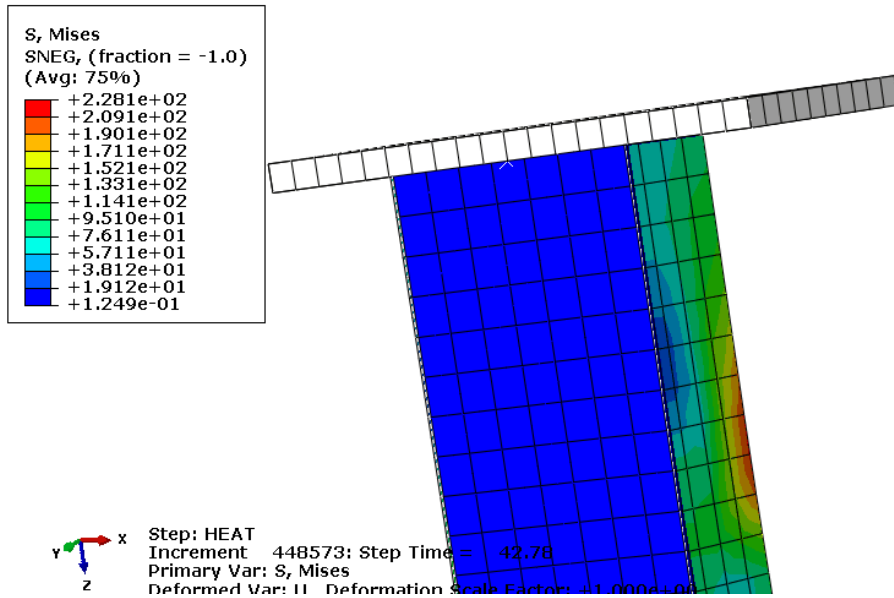
Figure 6.9. CFT column after load transferred from steel tube to concrete

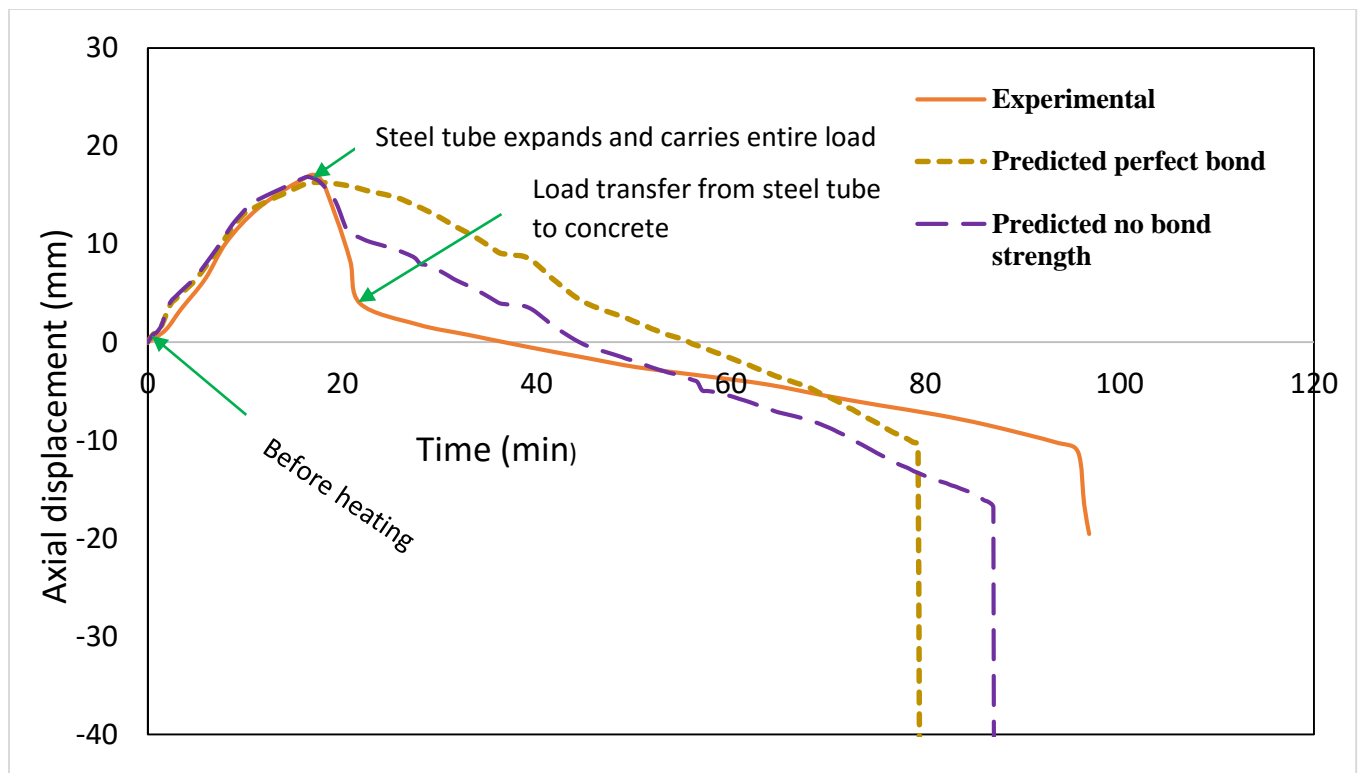The Positions of the above CFT column is shown in the figure

Figure 6.10. Axial displacement vs Time of column SQ20, showing the transfer of load from steel tube to concrete

Chapter 7

Parametric Studies

7.1. Parametric study on very slender column subjected to rapid and gradual fire:

Structural behavior of square CFT columns under two different fire intensities is studied. In the high intensity fire, the steel temperature rises to 600ºC and 800ºC in 22 and 48 minutes respectively. But in low intensity fire, the steel temperature rises to 600ºC and 800ºC in 70 and 110 minutes respectively. The slenderness ratios of the columns varied between 45 and 130. The thickness of steel tube varied from 4mm to 8 mm. An initial geometric imperfection of L/1000 is assumed.

It was observed that the column subjected to lower intensity fire sustain the applied load for longer duration than a similar column subjected to high intensity fire. The temperature difference between the steel tube and the concrete core is less in low intensity fire compared to high intensity fire. Also, it was observed that the temperatures of steel tube at failure is almost same irrespective of the fire intensity. Figures 7.1 and 7.2 show the axial displacement vs time and steel tube temperature vs time plots for two identical slender CFT columns which are exposed to gradual and rapidly growing fires, respectively. The steel tube thickness varies from 4mm to 8 mm in both cases. As the column is very slender, the load carrying capacity of the column suddenly falls after a certain period of fire exposure.

Figures 7.1 and 7.2 show that there is the duration of fire before failure changes significantly (approximately 200% - 300%) as the fire intensity changes. The corresponding steel

tube temperatures, however, at the time of failure were almost equal in the two cases. The temperatures at failure for 4mm thick steel tube columns were 655°C and 675°C (5% difference) in case of gradual and rapidly growing fires, respectively. For 6mm thick steel tube the temperatures were 689°C and 700°C (3% difference), respectively. The corresponding differences between concrete temperatures were approximately 54% and 57 %. This clearly shows that the column capacity is very strongly correlated with the steel temperature irrespective of the temperature distribution in the column cross-section.
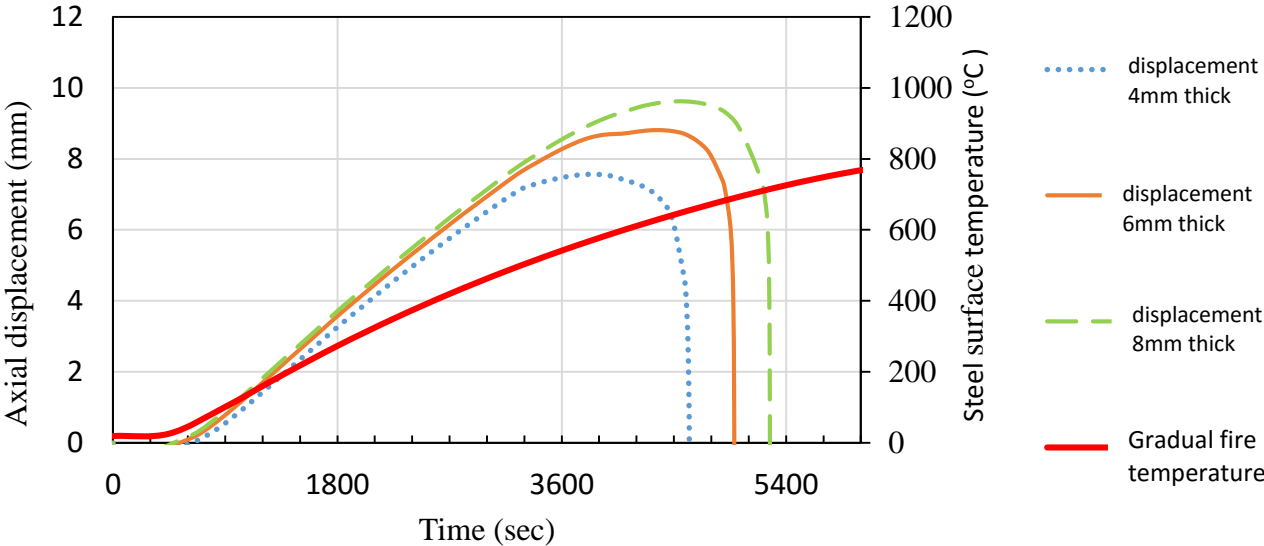
Figure 7.1. Axial displacement vs time under gradual fire
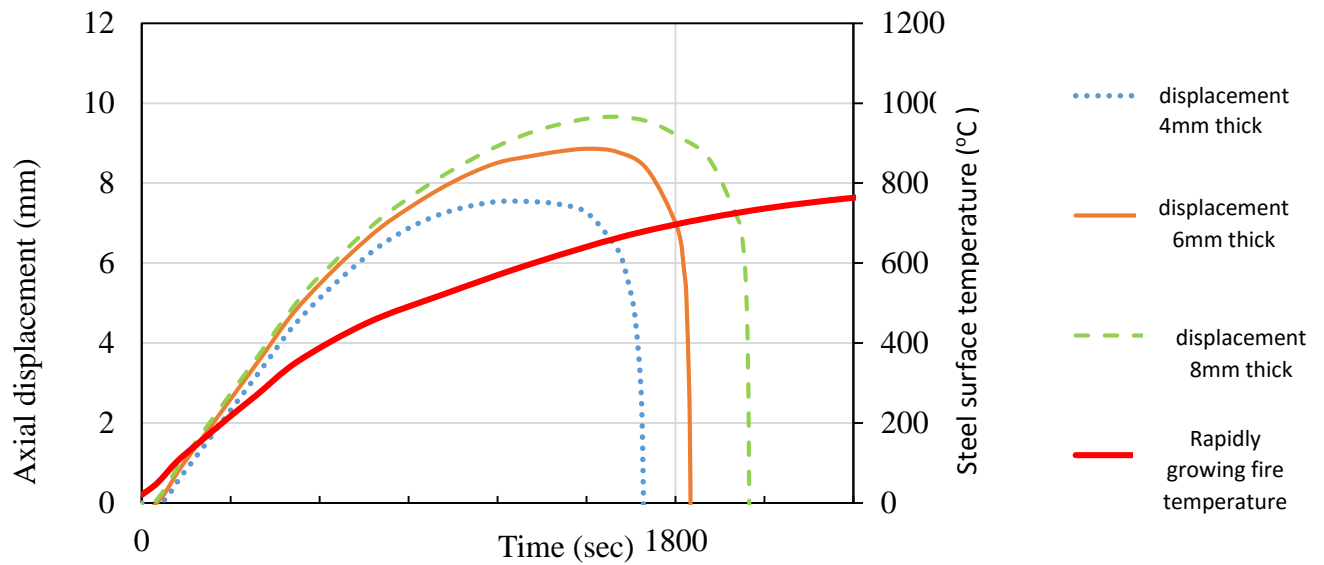
Figure 7.2. Axial displacement vs time under rapidly growing fire

7.2. Parametric study on 250*250mm column with fire protection - Comparison with the Eurocode

The design equations given in the Eurocode predicts the capacity of the CFT column at elevated temperatures. But the steel concrete interface is assumed to be perfectly bonded, which doesn't hold good when compared with experimental results.

A limited Parametric study was carried out to understand how the column behavior changes as the geometry of the column changes. Also the eventual use of this exercise is to develop a design guideline for such columns. CFT column of square cross-section with outer dimension 250x250mm was subjected to 10 hr of fire, where the temperature rises from 20 $^{\circ}$C to around 1000°C at the end of 10th hr.
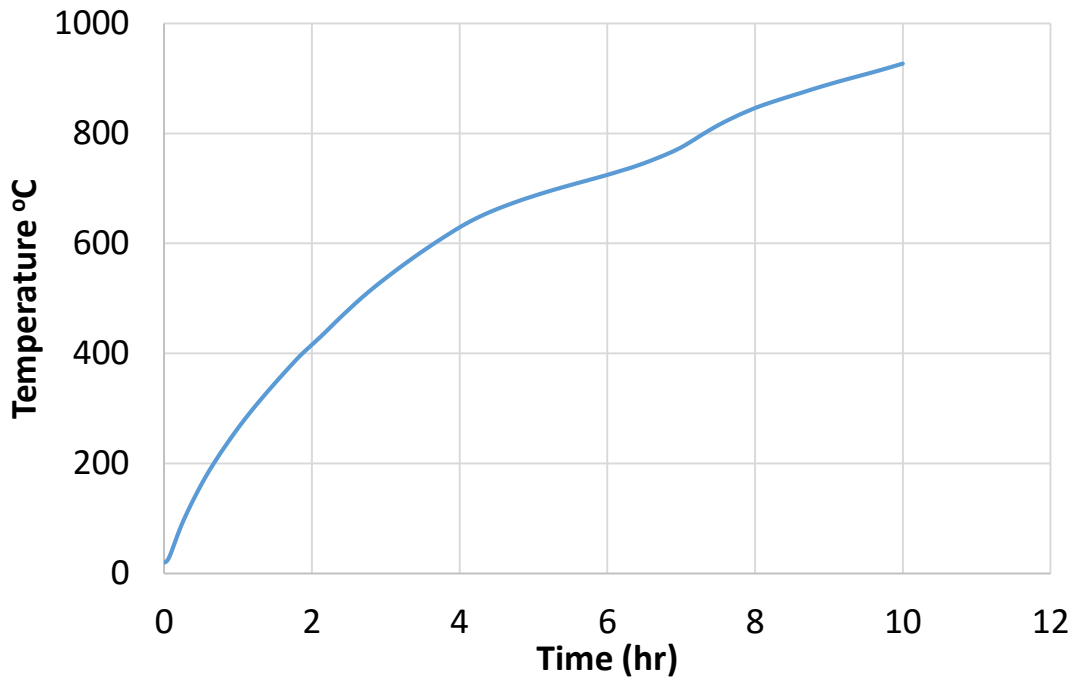
Figure 7.3. Temperature vs Time curve of column subjected to 10 hr fire

Compressive strength of concrete is assumed to be 40 MPa and steel yield strength is assumed to be 350 MPa. The length of the CFT columns that are used are 1000 mm, 2000 mm, 4000 mm, and 8000 mm, steel tube thickness of is taken as 4mm. All the simulations in the parametric study are conducted using the numerical model developed and validated in the above section. The interface is modeled as contact with zero bond strength. The load required for the failure of each column at temperatures 400 °C, 500 °C, 600 °C, 700 °C are simulated and compared with the column strengths predicted using the Eurocode (1994-1-2).
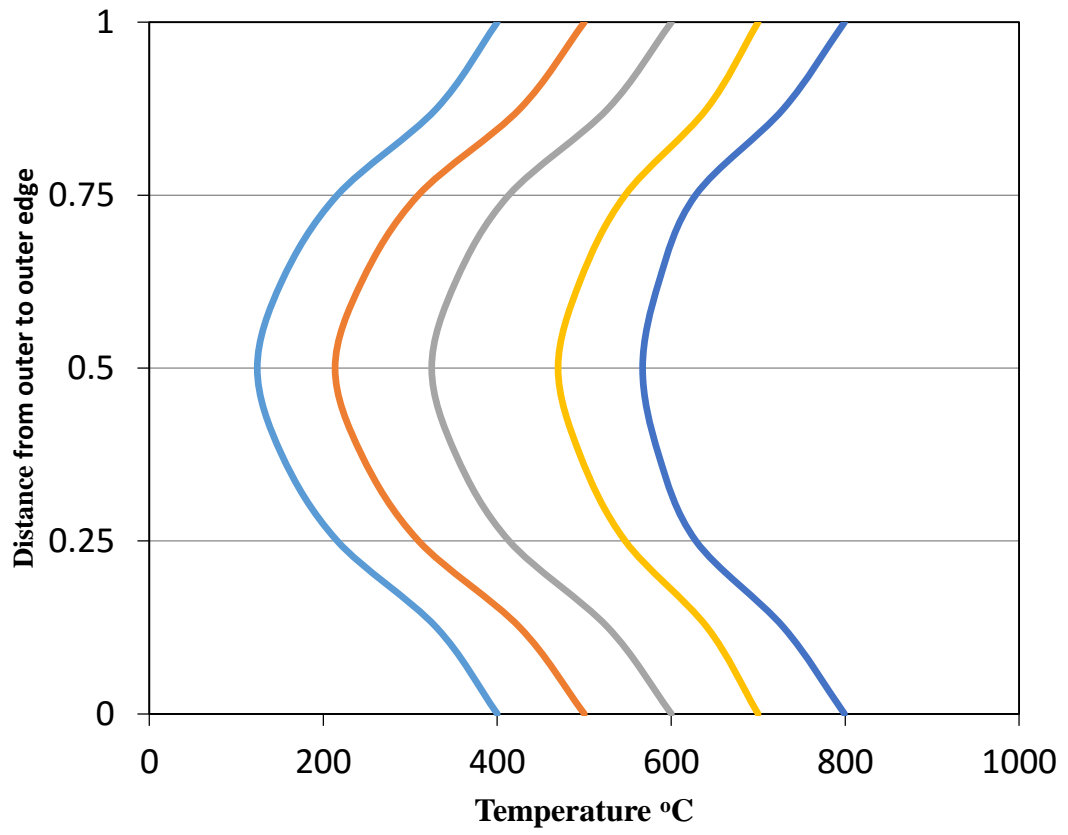
Figure 7.4. Temperature variation along the column cross-section

Figure 7.5. Comparisons of Normalized strengths against Eurocode at steel temperature of 400^0C
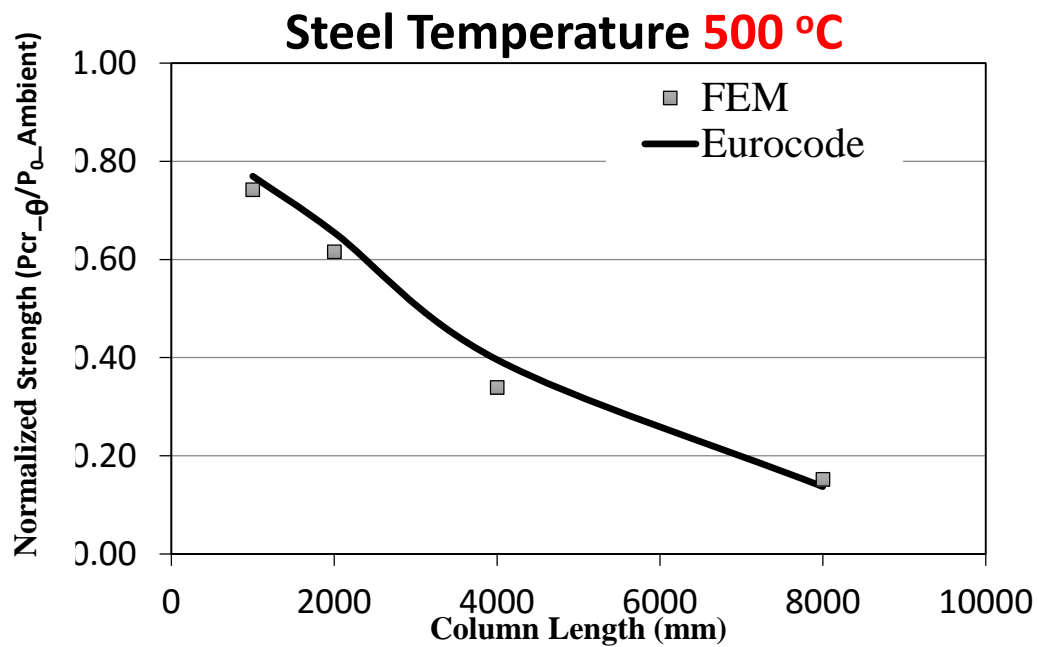
Figure 7.6. Comparisons of Normalized stregths against Eurocode at steel temperature of 500^0C
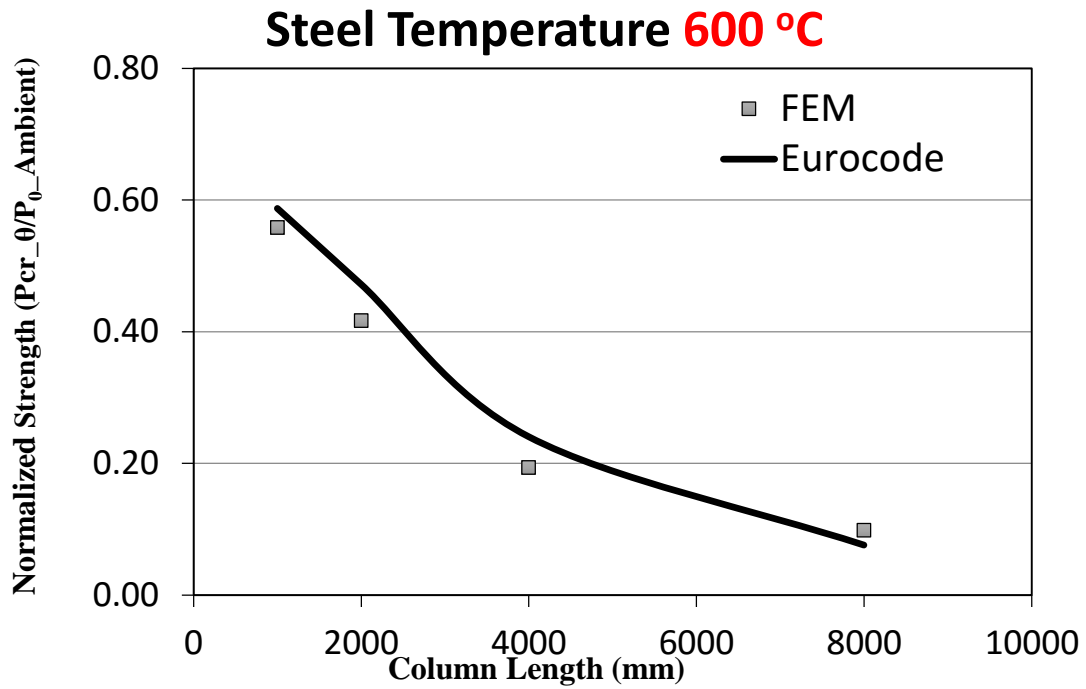
Figure 7.7. Comparisons of Normalized strengths against Eurocode at steel temperature of 600^0C
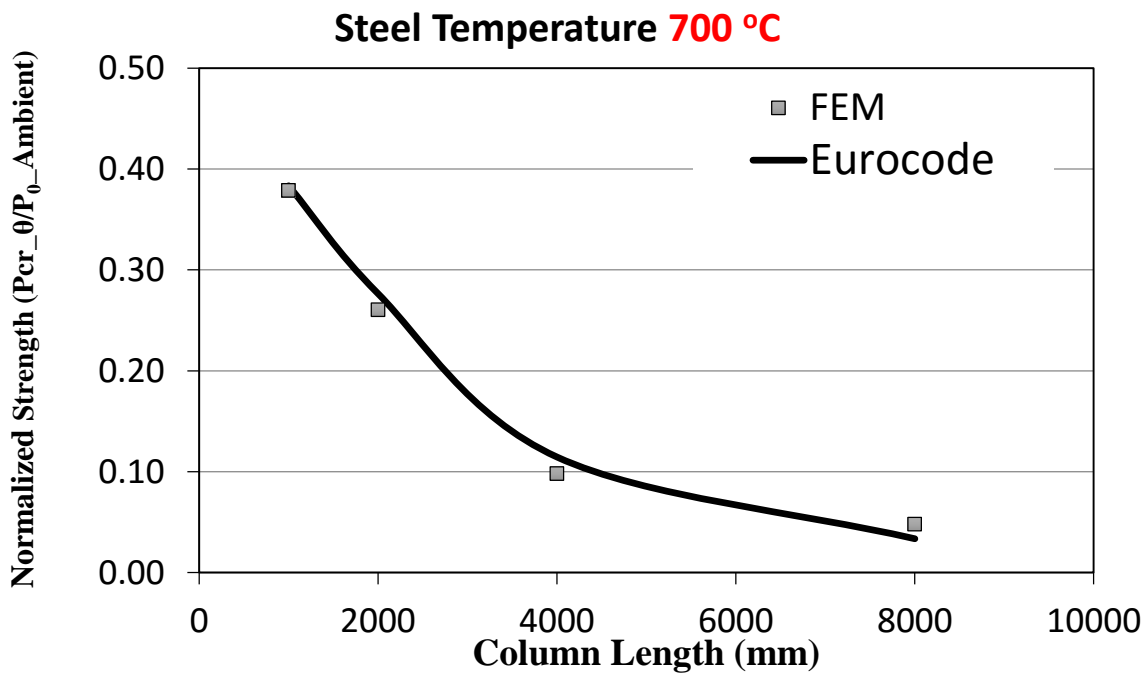
Figure 7.8. Comparisons of Normalized strengths against Eurocode at steel temperature of 700^0C

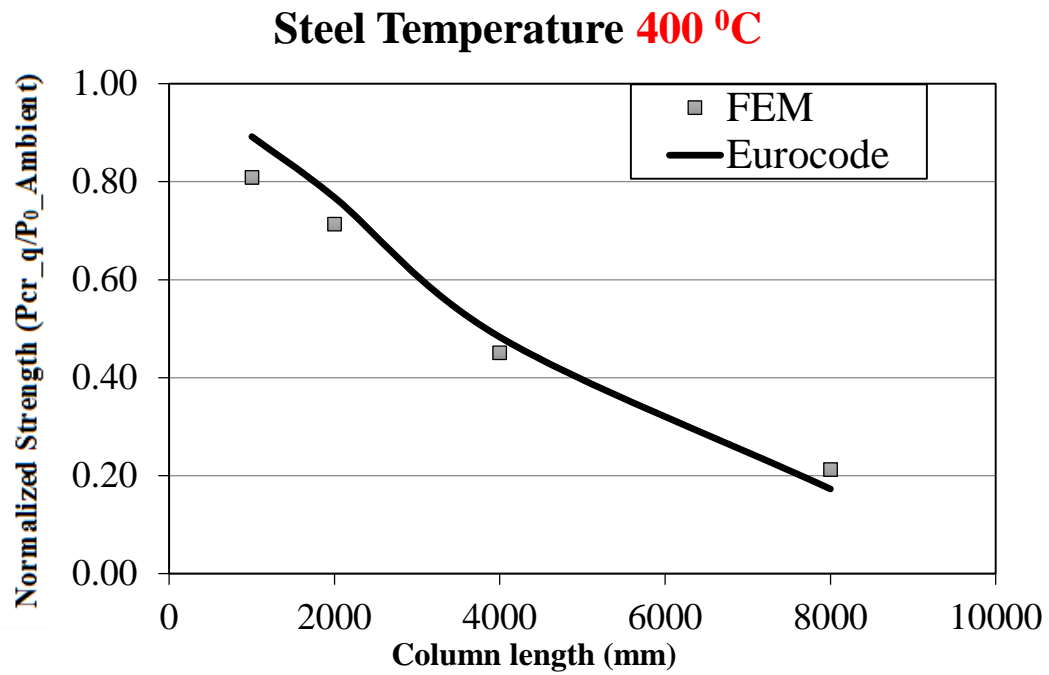The column capacities obtained from the parametric studies are compared with the values

obtained from the Eurocode. The normalized strengths (i.e, load at particular temperature to

ambient capacity) of both the Eurocode and the FEM analysis are compared for different lengths

at the particular temperatures. Column capacities obtained from the FEM analysis predicts less

capacities than the Eurocode. But the capacities for the column of 8000mm length predicted

higher values than the Eurocode. Based on the results provided above, a 3-D plot between

column length, steel temperature and column load capacity is plotted in figure 7.9. More detailed

parametric study is required to develop similar plots for column of different cross-sections, tube

thickness, fire intensities etc. Regression analysis using this data base will eventually be used to

develop a comprehensive design equation for CFT column at elevated temperatures.
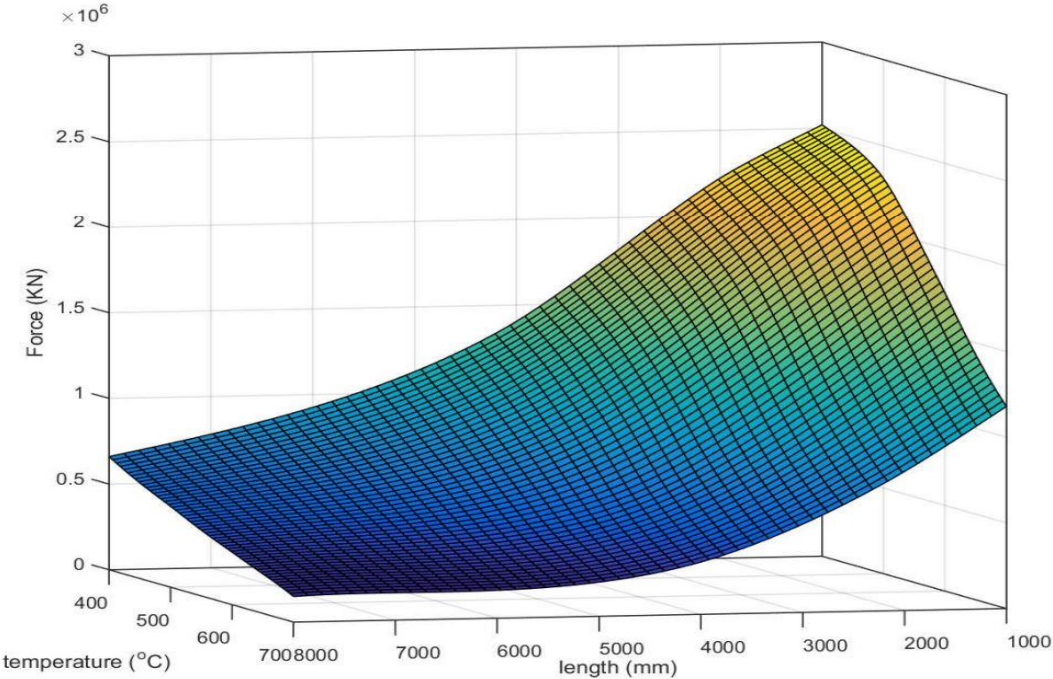
Figure 7.9. Column failure surface developed using the simulation results

Chapter 8

Summary and Conclusions

In this thesis, fire behavior of axially loaded concrete filled tubular columns is investigated through numerical modelling. A three dimensional finite element model was developed to predict the structural behavior of axially loaded CFT columns. The accuracy of the numerical model was validated against the experimental results available in the literature. Square and circular CFT columns were modelled and checked for their accuracy in predicting the column capacities. Some of the conclusions that are drawn from the numerical models and parametric studies are as follows.

- Numerical model showed a very good agreement with the experimental tests in case of the circular columns at ambient temperature

- The results obtained at the ambient temperature has the values which are greater than the experimental values. Therefore, the capacities are over-predicted.

- The failure of the column takes place as soon as the steel temperature reaches a particular value, regardless of the applied fire intensity.

- The fire resistance of the CFT column depends on the geometric imperfection, fire resistance rating increases as the imperfection decreases.

- Due to this temperature variation in the radial direction, CFT columns are found to be subjected to the hoop stresses, which are not observed in typical steel columns at elevated temperatures. These stresses make the overall compressive load carrying capacity of the column at elevated temperature depend on the tensile strength of concrete.

- The interface between the steel and concrete plays an important role in predicting behavior of CFT columns. The interaction with zero bond strength between the steel and concrete holds good and resembles with the deformed shape of experimental tests.

- If the bond between the steel and concrete is perfect i.e, rigid then the local buckling of steel tube doesn't takes place, also the predicted fire resistance will be lower.

- The friction coefficient between the steel and concrete surface doesn't have any influence on the column fire behavior.

- The fire resistance increases by around 7-8% if we decrease the imperfection factor from L/1500 to L/7500.

- Parametric studies are done to develop a general design equation in predicting the fire behavior of CFT column. The obtained results are validated against the Eurocode design capacities. The predicted column capacities are found to be less than the Eurocode column capacities.

References

ABAQUS. ABAQUS/Standard version 6.13 user's manual: Volumes I-III. Pawtucket, Rhode Island: Hibbit, Karlsson & Sorenson, Inc.; 2005.

Ana Espinos capilla (2012), "Numerical analysis of the fire resistance of Circular and Elliptical Slender Concrete filled Tubular Columns", PhD Dissertation, Department of Construction Engineering and Civil Engineering Projects, University at politecnica De Valencia, Spain.

ASTM (1999). "Standard Test methods and Definitions for Mechanical Testing of Steel Products," A370-97a, west Conshohocken, PA.

ASTM. Standard test methods for fire tests of building construction and materials, E119. W. Conshohocken (PA): American Society for Testing and Materials: 2003.

ASTM (2003) "Standard Test methods for fire tests of building construction and materials" E119, American society of testing and materials, W. Conshohocken, PA.

CEN. EN 1994-1-2, Eurocode 4: Design of composite steel and concrete structures. Part 1-2: General rules – Structural fire design. Brussels, Belgium: Comite Europeen de Normalisation; 2005.

CEN. EN 1993-1-2, Eurocode 3: Design of steel structures. Part 1-2 General rules – Structural fire design. Brussels, Belgium: Comite Europeen de Normalisation; 2005.

CEN. EN 1992-1-2, Eurocode 2: Design of concrete structures. Part 1-2: General rules – Structural structures. Part 1-2: General rules – Structural fire design. Brussels, Belgium: Comite Europeen de Normalisation; 2004.

Chabot, M. , and Lie T. T. ,(1992), "Experimental studies on the fire resistance of hollow steel columns filled with bar-reinforced concrete." IRC internal Rep. NO 628, National Research Council of Canada, Institute for Research in Construction, Ottawa, Ontario.

Han LH. Fire performance of concrete filled steel tubular beam-columns, Journal of Constructional Steel Research 2001:57:695-709

Han LH, Xu L, Fire resistance of concrete filled steel tubes. In: Xiao Y, Mahin SA, editors, Comp. and Hybrid Struc. Los Angeles, CA: ASCCS: 2000.p. 247-54.

Han LH, Yang YF, Xu L. An experimental study and calculation on the fire resistance of concrete filled SHS columns. Journal of Constructional Steel Research 2003; 59(4):427-452.

Han LH, Zhao XL, Yang YF, Feng JB. Experimental study and calculation of concrete-filled hollow steel columns. Journal of Structural Engineering, ASCE 2003; 129(3):346-356.

Han LH, Chen F, Lia FY, Tao Z, Uy B. Fire performance of concrete filled stainless steel tubular columns. Eng Struct 2013;56: 165-81.

Han LH, Yao GH, Tao Z. Behaviors of concrete-filled steel tubular members subjected to combined loading. Thin Wall Struct 2007; 45(6): 600-19.

Han LH, Wang WH, Yu HX. Experimental behavior of reinforced concrete (RC) beam to concrete-filled steel tubular (CFST) column frames subjected to ISO-834 standard fire. Eng Struct 2010; 32(10): 3130-44.

Hong. S. Fundamental Behavior and Stability of CFT Columns under fire loading, Ph.D. dissertation, West Lafayette (IN): School of Civil Eng., Purdue University: May 2007

Hong. S, Varma AH. Analytical modeling of the standard fire behavior of loaded DFT columns. Journal of Constructional Research 2009; 65:54-69.

Huo JS, He YM, Chen BS. Experimental study on impact behavior of concrete-filled steel tubes at elevated temperatures upto 800ºC. Mater Struct 2013.

ISO-834, Fire resistance tests – Elements of building construction. International standards ISO 834. Geneva, Switzerland: 1975.

Kodur VKR. Guidelines for fire resistant design of concrete-filled steel HSS columns – state of art the art and research needs. Steel Structures 2007; 7:173-182.

Kodur VK. Design equations for evaluating the fire resistance of SFRC-filled HSSS columns. Journal of Structural Engineering 1998: 124(6): 671-7

Lie T. T. Kodur VK, (1994) ,"Fire resistance of circular steel columns filled with bar-reinforced concrete." J. Struct. Engg. ASCE, 120(5), 1489-1509.

Lie, T.T and Irwin, R. J. (1995), "Fire resistance of rectangular steel columns filled with bar-reinforced concrete" J. Struct. Engg. ASCE, 121(5), 797-805.

Liu FQ, Yang H, Zhang SM. Comparison of the fire resistance of concrete-filled SHS columns subjected to 3-sided and 4-sided exposure. In: 10th international conference on advances in steel concrete composite and hybrid structures 2012. P. 889-896.

Mao XY, Kodur VKR. Fire resistance of concrete encased columns under 3-and 4- sided heating. J Constuct Steel Res 2011; 44(6): 869-80.

Poh KW. Stress-strain –temperature relationships for structural steel. Journal of Materials in Civil Engineering 2001: 13(5):371-9.

Romero ML, Moliner V, Espinos A, Ibanez C, Hospitaler A. Fire behavior of axially loaded slender high strength concrete-filled tubular columns. Journal of Constructional Steel Research 2011: 67(12): 1953-1965.

Schaumann P, Kodur VKR, Bahr O. Fire behavior of hollow structural section steel columns filled with high strength concrete. J Construct Steel Res 2009; 65(8): 1794-802.

Wang YC. A simple method for calculating the fire resistance of concrete-filled CHS columns. Journal of Constructional Steel Research 2000; 54:365-386.

Wang, Y.C. (2002). Steel and Composite Structures: Behavior and design for fire safety. SPON Press.

Yang H, Liu FQ, Zhang SM, Lv XT. Experimental investigation of concrete filled square hollow section columns subjected to non-uniform exposure. Eng Struct 2013; 48: 292-312.

Yang YF, Han LH. Experiments on rectangular concrete filled steel tubes loaded axially on a partially stressed cross-sectional area. J Construct Steel Res 2009; 65(8):1617-30.